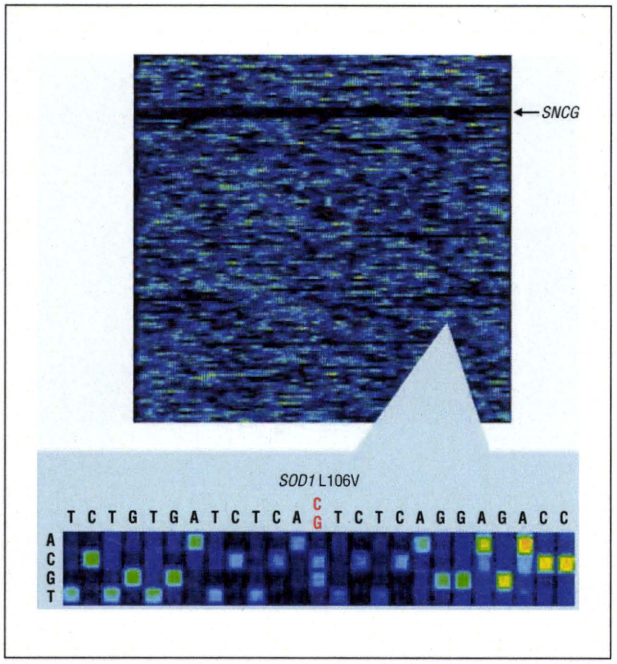

Figure 2. Whole view of microarray TKYALS01. A heterozygous point mutation of *SOD1*, L106V, was unambiguously identified.

METHODS

DESIGN OF MICROARRAYS

We have designed a microarray, TKYALS01, that primarily focuses on the causative genes of and genes related to ALS (**Table 1**). The sequences tiled on the microarray included the sequences of all of the exons and 12 flanking base pairs (bp) of the splice junctions. Promoter sequences were also included in the tiled sequences for genes whose expression levels were presumed to modify the disease processes.[4,5] In addition, another microarray, TKYPD01, was designed to focus on genes relevant to Parkinson disease, autosomal-dominant hereditary spastic paraplegias, and adrenoleukodystrophy (data not shown).

Because the principle of the resequencing microarray is based on sequencing by hybridization (SBH), it is crucially important to avoid cross-hybridization to increase the accuracy of resequencing. For this purpose, we conducted an "in silico" screening to compare the tiled sequences with a sliding 25-nucleotide window to detect the sequences with an identity exceeding 22 bases in the tiled sequences and optimized the design of the microarrays and polymerase chain reaction (PCR) primers.

PARTICIPANTS

Thirty-five patients with sporadic ALS and 10 patients with familial ALS, 7 with autosomal dominant mode of inheritance and 3 with affected siblings, were enrolled in this study. The diagnosis of ALS was based on El Escorial and the revised Airlie House diagnostic criteria. A total of 238 control genomic DNA samples were also used.

Thirty-six genomic DNA samples with previously determined mutations of *SOD1* (OMIM 147450), the causative gene of familial ALS,[6-9] or those of *ABCD1* (OMIM 300371), the causative gene of adrenoleukodystrophy,[10-13] were anonymized and subjected to analysis without prior information on the mutations.

All of the genomic DNA samples were obtained with written informed consent, and this research was approved by the institutional review board of the University of Tokyo.

PROCEDURES

Specific PCR primers were designed using the Primer3 Web site (http://frodo.wi.mit.edu/cgi-bin/primer3/primer3_www.cgi) (**eTable**, http://www.archneurol.com). Touch-down PCR protocols were used to enhance the specificity of PCR amplification (eTable). Each PCR product was quantified using PicoGreen (Molecular Probes, Eugene, Oregon), pooled equimolarly into 1 tube using a robotic system, BioMek FX (Beckman Coulter, Fullerton, California), and subjected to SBH according to the manufacturer's instructions (Affymetrix, Santa Clara, California) (**Figure 1**). The undetermined base calls were further analyzed by manual inspection of the signals. The resequencing of *ANG* (OMIM 105850) and the confirmation of all of the sequence variants determined by SBH were conducted by direct nucleotide sequence analysis using an automated DNA sequencer and BigDye Terminator version 3.1 (Applied Biosystems, Foster City, California). Analyses of frequency of variants in the controls were conducted by denatured high-performance liquid chromatography (Transgenomics, Omaha, Nebraska).

RESULTS

ESTABLISHMENT OF HIGH-THROUGHPUT COMPREHENSIVE RESEQUENCING SYSTEM

To evaluate the signal-to-noise ratio, all of the PCR amplicons for TKYALS01 except those for *SNCG* were subjected to hybridization to TKYALS01 and scanning. Simultaneous hybridization of the mixed PCR amplicons did not interfere with the signals and *SOD1* mutations were unambiguously identified (**Figure 2**). Furthermore, the areas where the probes for *SNCG* were tiled did not show any detectable signals, indicating that cross-hybridization was negligible.

As shown in **Figure 3**A, all of the point mutations were correctly identified, confirming the accuracy of SBH for detection of point mutations. The locations of the hemizygous *ABCD1* insertion/deletion mutations were also easily identified because the signals of the insertion/deletion sites and surrounding probes were undetectable (Figure 3B). Determination of the exact base changes required direct nucleotide sequence analysis. In contrast, none of the 4 heterozygous insertion/deletion mutations of *SOD1* were unambiguously detected without prior information on the mutations. Only the *SOD1* heterozygous deletion mutation del429TT was detectable by carefully evaluating the signal intensities (Figure 3C) because the signal intensities were moderately decreased at the deletion sites and the 12 flanking bases (Figure 3D).

By employing robotics to manipulate numerous PCR reactions, the resequencing of as many as 271 625 bp was easily accomplished in 3 working days with a total of 271 445 bp (99.93%) correctly called, confirming the high throughput of this system.

COMPREHENSIVE RESEQUENCING OF GENES RELEVANT TO ALS

The molecular diagnosis of 10 patients with familial ALS using this system revealed 2 *SOD1* mutations, including 1 novel mutation, K3E (**Figure 4**A), and 1 previously

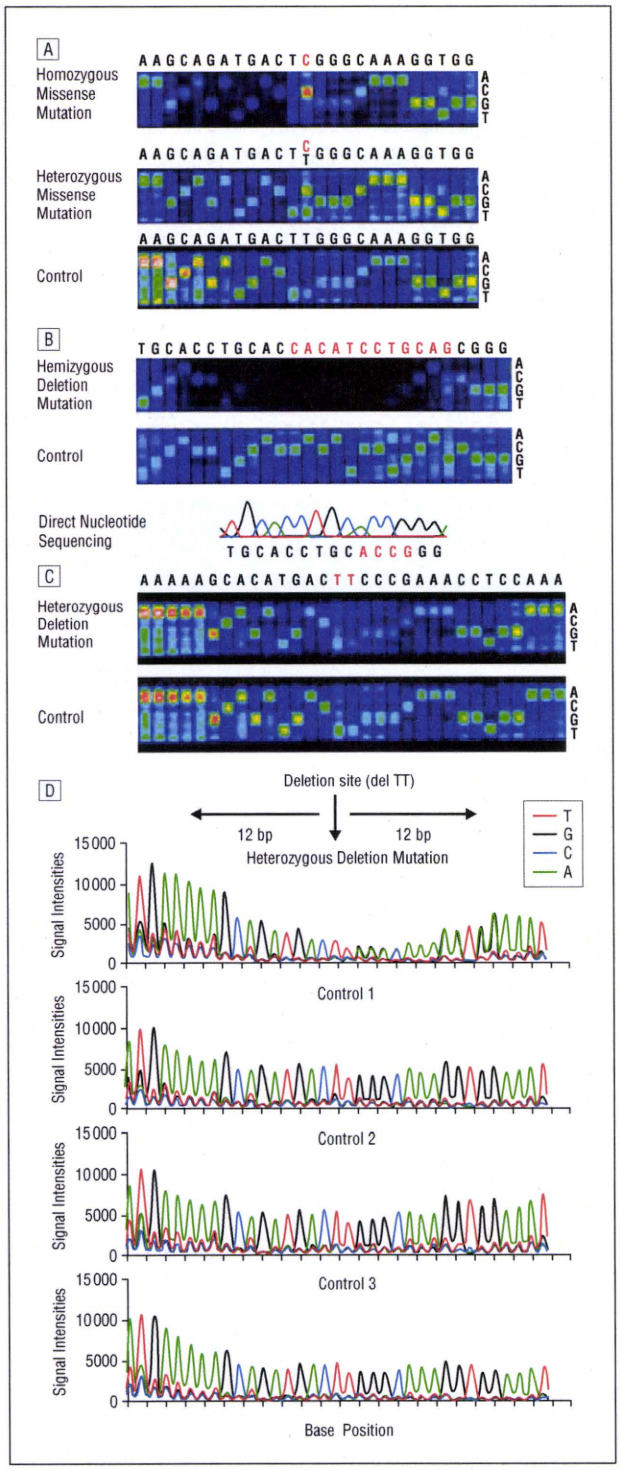

Figure 3. Validation of accuracy of sequence determination. A, Scan images of homozygous and heterozygous *SOD1* L126S mutations. Each column shows a base position, and each row shows a base call (the determination of base(s) at each position). In the center position, the base call was T in the control, whereas in the patients, the base calls were homozygous C (upper panel) or heterozygous C/T (middle panel). B, Scan image of hemizygous *ABCD1* del2146-2157 mutation. Signals of the deletion site and surrounding probes were virtually undetectable. C, Scan image of heterozygous *SOD1* L129 (del459TT) mutation. The base calls at the mutation site of the patient were the same as those of the control. The probes at and around the mutation site, however, showed decreased signal intensities compared with those of the controls. D, Signal intensities at and around the deletion site of heterozygous *SOD1* L129 (del459TT) mutation. Signal intensities at the deletion site (del TT) and the flanking bases were approximately half those of the controls. bp indicates base pairs.

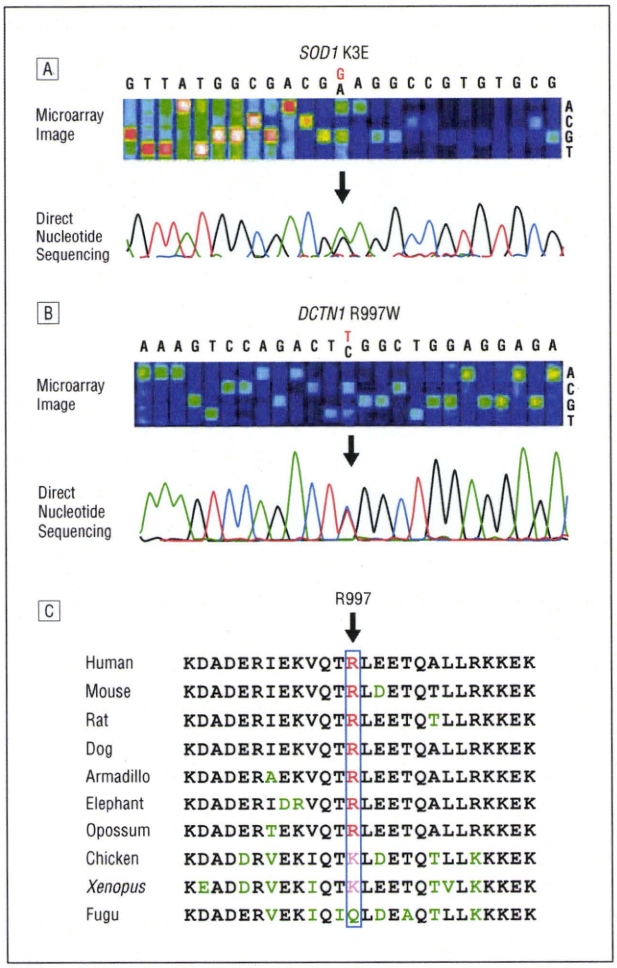

Figure 4. Novel mutations identified in patients with familial and sporadic amyotrophic lateral sclerosis (ALS). A, Scan image of heterozygous *SOD1* K3E point mutation. The A to G heterozygous point mutation was identified in a patient with familial ALS. B, Scan image of heterozygous *DCTN1* R997W point mutation. The C to T heterozygous point mutation was identified in a patient with sporadic ALS. C, Conservation of *DCTN1* amino acid sequences in different animal species. The arginine residue at codon 997 is highly conserved among species (shown in red), including a synonymous basic amino acid, lysine (shown in pink), in chicken and *Xenopus laevis*. Nonconserved amino acids are shown in green.

identified mutation, I106V. The novel mutation was not identified in the 238 controls (476 chromosomes). The novel *SOD1* mutation was found in a 70-year-old man presenting with progressive distal-dominant muscle atrophy, weakness in all extremities, and positive Babinski signs.

In the 35 patients with sporadic ALS, we identified a previously known *SOD1* mutation, S134N, and a novel putative pathogenic *DCTN1* (OMIM 601143) mutation, R997W (Figure 4B). These mutations were not present in the 238 controls (476 chromosomes). The amino acid residue R997 of *DCTN1* was located in a region conserved among different animal species (Figure 4C). The patient with the *DCTN1* mutation was a 68-year-old man presenting with progressive muscle atrophy, weakness in all of his extremities, and postural tremor in the upper extremities, with onset at the age of 67 years. Findings from neurological examination on admission at 68 years of age revealed diffuse muscle atrophy, weakness,

Table 2. Summary of Novel Variants Identified by Comprehensive Resequencing in 35 Patients With Sporadic ALS

Gene	Fragment	Position[a]	Base Call[b]	Category	Amino Acid Change
ALS2[c]	Exon 5	202447798	A/T	Coding nonsynonymous	Q435L
ALS2[c]	Exon 18	202417029	C/A	Coding nonsynonymous	P1016T
ANG[c]	Exon 2	20231781	A/G	Coding nonsynonymous	N49S
VEGF	Exon 6	43856523	G/A	Coding nonsynonymous	V167I
DCTN1	Exon 18	74506526	T/C	Coding synonymous	
RNF19[c]	Exon 7	101346118	G/A	Coding synonymous	
VEGF[c]	Exon 3	43853233	G/A	Coding synonymous	
DCTN1	Exon 1	74519378	T/C	5′ Untranslated region	
VEGF	Promoter	43846646	G/A	Promoter	

Abbreviation: ALS, amyotrophic lateral sclerosis.
[a]Positions were based on the University of California Santa Cruz genome browser hg17.
[b]The determination of base(s) at each position.
[c]These variants were present only in patients with sporadic ALS.

Table 3. Summary of Known SNPs Identified by Comprehensive Resequencing in 35 Patients With Sporadic ALS

Gene	SNP ID	Category
ALS2	rs3219156	Coding nonsynonymous
ALS2	rs41308814	Coding nonsynonymous
ALS2	rs41308840	Coding nonsynonymous
ALS2	rs41309046	Coding nonsynonymous
ADAR2	rs1051367	Coding synonymous
ALS2	rs2276615	Coding synonymous
ALS2	rs3219161	Coding synonymous
ALS2	rs3219168	Coding synonymous
SLC1A2	rs752949	Coding synonymous
SLC1A2	rs1042113	Coding synonymous
VEGF	rs699947	Promoter
VEGF	rs1005230	Promoter
VEGF	rs833061	Promoter
VEGF	rs13207351	Promoter
VEGF	rs1570360	Promoter
VEGF	rs2010963	Promoter
VEGF	rs25648	Promoter
ALS2	rs2276614	5′UTR
ALS2	rs3219169	Intron
ALS2	rs3219153	Intron
CNTF	rs1800169	Intron
SLC1A2	rs2273689	Intron

Abbreviations: ALS, amyotrophic lateral sclerosis; SNP ID, single-nucleotide polymorphism identification; UTR, untranslated region.

fasciculation, and hyporeflexia in all extremities. Weakness of neck flexion was also noted. Observation of his intelligence was normal. Neither bulbar sign nor pyramidal sign was recognized. Electromyography showed diffuse active neurogenic changes compatible with progressive lower motor neuron degeneration. His parents remained healthy beyond 80 years of age.

The comprehensive analysis of the 35 patients with sporadic ALS also revealed 31 sequence alterations in addition to the 2 mutations described above (**Table 2** and **Table 3**). Nine of the 31 variants (29%) were novel (**Figure 5**A), including 4 nonsynonymous heterozygous variants consisting of 2 in *ALS2* (OMIM 606352), 1 in *ANG*, and 1 in *VEGF* (OMIM 192240) (Figure 5B) that were present in the ALS patients but not in 238 controls (476 chromosomes).

COMMENT

The effect of the microarray-based high-throughput resequencing system is 3-fold. First, it enables comprehensive mutational analyses of multiple causative genes for the diagnosis of familial cases. Because of nonallelic genetic heterogeneities and clinical variability, it is often difficult to focus on particular genes depending solely on the phenotypes. In this situation, the comprehensive analysis of causative genes is often superior to categorical approaches based on clinical information. The second effect is the identification of mutations in causative genes in sporadic cases (Figure 4). Thus, comprehensive resequencing of the causative genes may reveal mutations with reduced penetrance or de novo mutations in a portion of patients with sporadic ALS. The system has a great advantage in screening numerous genes in many patients with sporadic ALS.

The third effect is the discovery of rare variants potentially involved in disease susceptibility. The current approaches for identifying genetic risks of ALS are mainly based on GWAS employing common single-nucleotide polymorphisms, which generally provide relatively low odds ratios.[14,15] The extensive resequencing of relevant genes is expected to complement GWAS by identifying rare variants that contribute to the development of diseases with substantially high odds ratios.[16-19] Large-scale resequencing projects to uncover functional and regulatory variants are currently in progress, identifying numerous novel variants.[20] Indeed, nonsynonymous heterozygous variants in *ALS2*, *ANG*, and *VEGF* are overrepresented in patients with ALS (Figure 5B). To confirm the significance of these rare variants in disease pathogenesis, large-scale case-control studies and functional analyses of individual mutant proteins will be required.

The advantage of SBH lies in resequencing particular sets of genes. Once the microarrays are designed, the sequencing is inexpensive and the system can be efficiently used for the repetitive interrogation of the same genome region. To further enhance the throughput of the resequencing system based on SBH, improvement in the detection capability for heterozygous insertion/deletion mutations is required. It seems theoretically possible to

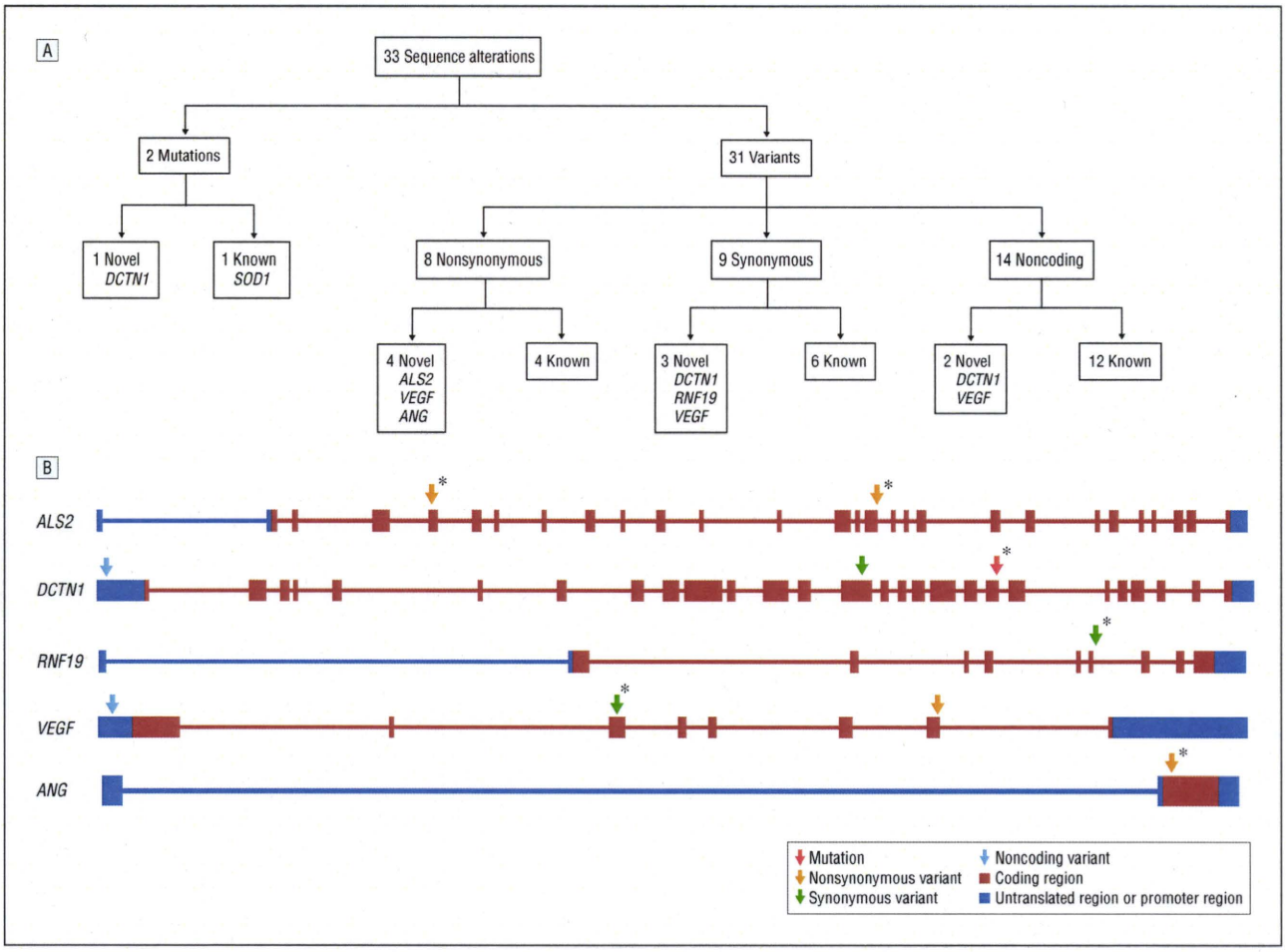

Figure 5. Summary of comprehensive resequencing of causative and disease-related genes in patients with sporadic amyotrophic lateral sclerosis (ALS). A, Classification of sequence alterations identified in this study. Thirty-three sequence alterations including 2 mutations and 31 variants were found in 1 megabase resequencing. Of the 31 variants, 9 (29%) were novel. These novel variants were listed in neither the Single Nucleotide Polymorphism database (http://www.ncbi.nlm.nih.gov/SNP/index.html) nor the Japanese Single Nucleotide Polymorphism database (http://snp.ims.u-tokyo.ac.jp/). B, Locations of novel mutations and variants. Novel mutations, nonsynonymous variants, synonymous variants, and noncoding variants are shown in arrows with respective colors at each location in the corresponding genes. The structure of each gene was obtained from Entrez Gene (http://www.ncbi.nlm.nih.gov/entrez/query.fcgi?db=gene). * Indicates variants that were only found in patients with sporadic ALS.

overcome this issue by optimizing hybridization conditions and detecting changes in the signal intensity patterns.[21]

The DNA microarray–based high-throughput resequencing system for comprehensive analysis of causative and disease-related genes contributes to the identification of causative mutations not only in familial ALS cases but also in some sporadic cases with low-penetrant mutations or de novo mutations, and to the identification of numerous rare variations potentially associated with diseases. This system serves as a milestone for translating the technological innovation of high-throughput resequencing directly into clinical practice.

Accepted for Publication: March 21, 2008.
Author Affiliations: Departments of Neurology, Graduate School of Medicine, University of Tokyo, Tokyo (Drs Takahashi, Seki, Ishiura, Mitsui, Matsukawa, Kishino, Goto, and Tsuji), Brain Research Institute, Niigata University, Niigata (Drs Onodera and Nishizawa), and Tohoku University Graduate School of Medicine, Sendai (Drs Aoki and Itoyama); Division of Genomics Research, Life Science Research Center, Gifu University, Gifu (Dr Shimozawa); Geriatric Neuroscience (Neuropathology), Tokyo Metropolitan Institute of Gerontology, Tokyo (Dr Murayama); Department of Pediatrics, Gifu University School of Medicine, Gifu (Dr Suzuki); and Department of Neurology, Nagoya University Graduate School of Medicine, Nagoya, Japan (Dr Sobue).

Correspondence: Shoji Tsuji, MD, PhD, Department of Neurology, Graduate School of Medicine, University of Tokyo, Hongo 7-3-1, Bunkyo-ku, Tokyo 113-8655, Japan (tsuji@m.u-tokyo.ac.jp).

Author Contributions: Dr Tsuji had full access to all of the data in the study and takes responsibility for the integrity of the data and the accuracy of the data analysis. *Study concept and design:* Murayama, Itoyama, Goto, and Tsuji. *Acquisition of data:* Takahashi, Seki, Matsukawa, Kishino, Aoki, Shimozawa, Murayama, Suzuki, Sobue, Nishizawa, and Goto. *Analysis and interpretation of data:* Takahashi, Ishiura, Mitsui, Goto, and Tsuji. *Drafting of the manuscript:* Takahashi, Seki, Matsukawa, Kishino, Aoki, Itoyama, Suzuki, Sobue, Nishizawa, Goto, and Tsuji. *Critical revision of the manuscript for important intellec-*

tual content: Takahashi, Ishiura, Mitsui, Onodera, Shimozawa, Murayama, Goto, and Tsuji. *Obtained funding:* Tsuji. *Administrative, technical, and material support:* Takahashi, Seki, Ishiura, Kishino, Aoki, Shimozawa, Murayama, Suzuki, Sobue, Nishizawa, and Tsuji. *Study supervision:* Itoyama, Goto, and Tsuji.

Financial Disclosure: None reported.

Funding/Support: This study was supported in part by KAKENHI (Grant-in-Aid for Scientific Research) on Priority Areas; Applied Genomics, the 21st Century Center of Excellence Program, Center for Integrated Brain Medical Science, and Scientific Research (A) from the Ministry of Education, Culture, Sports, Science, and Technology of Japan; a Grant-in-Aid for the Research Committee for Ataxic Diseases of the Research on Measures for Intractable Diseases from the Ministry of Health, Labour, and Welfare, Japan; and a grant from the Takeda Foundation.

Additional Information: The eTable is available at http://www.archneurol.com.

REFERENCES

1. Kryukov GV, Pennacchio LA, Sunyaev SR. Most rare missense alleles are deleterious in humans: implications for complex disease and association studies. *Am J Hum Genet.* 2007;80(4):727-739.
2. Cutler DJ, Zwick ME, Carrasquillo MM, et al. High-throughput variation detection and genotyping using microarrays. *Genome Res.* 2001;11(11):1913-1925.
3. Warrington JA, Shah NA, Chen X, et al. New developments in high-throughput resequencing and variation detection using high density microarrays. *Hum Mutat.* 2002;19(4):402-409.
4. Wang CK, Chen CM, Chang CY, et al. alpha-Synuclein promoter RsaI T-to-C polymorphism and the risk of Parkinson's disease. *J Neural Transm.* 2006;113(10):1425-1433.
5. Mueller JC, Fuchs J, Hofer A, et al. Multiple regions of alpha-synuclein are associated with Parkinson's disease. *Ann Neurol.* 2005;57(4):535-541.
6. Rosen DR. Mutations in Cu/Zn superoxide dismutase gene are associated with familial amyotrophic lateral sclerosis. *Nature.* 1993;364(6435):362.
7. Pramatarova A, Goto J, Nanba E, et al. A two basepair deletion in the *SOD1* gene causes familial amyotrophic lateral sclerosis. *Hum Mol Genet.* 1994;3(11):2061-2062.
8. Kikugawa K, Nakano R, Inuzuka T, et al. A missense mutation in the *SOD1* gene in patients with amyotrophic lateral sclerosis from the Kii Peninsula and its vicinity, Japan. *Neurogenetics.* 1997;1(2):113-115.
9. Kato M, Aoki M, Ohta M, et al. Marked reduction of the Cu/Zn superoxide dismutase polypeptide in a case of familial amyotrophic lateral sclerosis with the homozygous mutation. *Neurosci Lett.* 2001;312(3):165-168.
10. Mosser J, Douar AM, Sarde CO, et al. Putative X-linked adrenoleukodystrophy gene shares unexpected homology with ABC transporters. *Nature.* 1993;361(6414):726-730.
11. Imamura A, Suzuki Y, Song XQ, et al. Prenatal diagnosis of adrenoleukodystrophy by means of mutation analysis. *Prenat Diagn.* 1996;16(3):259-261.
12. Imamura A, Suzuki Y, Song XQ, et al. Two novel missense mutations in the ATP-binding domain of the adrenoleukodystrophy gene: immunoblotting and immunocytological study of two patients. *Clin Genet.* 1997;51(5):322-325.
13. Takano H, Koike R, Onodera O, Sasaki R, Tsuji S. Mutational analysis and genotype-phenotype correlation of 29 unrelated Japanese patients with x-linked adrenoleukodystrophy. *Arch Neurol.* 1999;56(3):295-300.
14. Schymick JC, Scholz SW, Fung HC, et al. Genome-wide genotyping in amyotrophic lateral sclerosis and neurologically normal controls: first stage analysis and public release of data. *Lancet Neurol.* 2007;6(4):322-328.
15. van Es MA, van Vught PW, Blauw HM, et al. Genetic variation in DPP6 is associated with susceptibility to amyotrophic lateral sclerosis. *Nat Genet.* 2008;40(1):29-31.
16. Tantoso E, Yang Y, Li KB. How well do HapMap SNPs capture the untyped SNPs? *BMC Genomics.* 2006;7:238.
17. Coppola G, Geschwind DH. Technology insight: querying the genome with microarrays—progress and hope for neurological disease. *Nat Clin Pract Neurol.* 2006;2(3):147-158.
18. McKnight AJ, Savage DA, Patterson CC, Brady HR, Maxwell AP. Resequencing of the characterised CTGF gene to identify novel or known variants, and analysis of their association with diabetic nephropathy. *J Hum Genet.* 2006;51(4):383-386.
19. Lam CW, Yan MS, Law TY, et al. Resequencing the G6PT1 gene reveals a novel splicing mutation in a patient with glycogen storage disease type 1b. *Clin Chim Acta.* 2006;374(1-2):147-148.
20. Jorgenson E, Witte JS. A gene-centric approach to genome-wide association studies. *Nat Rev Genet.* 2006;7(11):885-891.
21. Karaman MW, Groshen S, Lee CC, Pike BL, Hacia JG. Comparisons of substitution, insertion and deletion probes for resequencing and mutational analysis using oligonucleotide microarrays. *Nucleic Acids Res.* 2005;33(3):e33.

J Neuropathol Exp Neurol

Vol. 67, No. 11
November 2008
pp. 1072–1083

ORIGINAL ARTICLE

Incidence and Extent of Lewy Body–Related α-Synucleinopathy in Aging Human Olfactory Bulb

Renpei Sengoku, MD, Yuko Saito, MD, PhD, Masako Ikemura, MD, PhD, Hiroyuki Hatsuta, MD, Yoshio Sakiyama, MD, PhD, Kazutomi Kanemaru, MD, PhD, Tomio Arai, MD, PhD, Motoji Sawabe, MD, PhD, Noriko Tanaka, PhD, Hideki Mochizuki, MD, PhD, Kiyoharu Inoue, MD, PhD, and Shigeo Murayama, MD, PhD

Abstract

We investigated the incidence and extent of Lewy body (LB)–related α-synucleinopathy (LBAS) in the olfactory bulb (OB) in 320 consecutive autopsy patients from a general geriatric hospital (mean age, 81.5 ± 8.5 years). Paraffin sections were immunostained with anti-phosphorylated α-synuclein, tyrosine hydroxylase, phosphorylated tau, and amyloid β antibodies. LBAS was found in 102 patients (31.9%) in the central nervous system, including the spinal cord; the OB was involved in 85 (26.6%). Among these 85 patients, 2 had LBAS only in the anterior olfactory nucleus, 14 in the peripheral OB only, and 69 in both areas. In 5 patients, Lewy bodies were found only in the OB by hematoxylin and eosin stain; 3 of these patients had Alzheimer disease, and all had LBAS. Very few tyrosine hydroxylase–immunoreactive periglomerular cells exhibited LBAS. All 35 LBAS patients with pigmentation loss in the substantia nigra had LBAS in the OB. LBAS in the amygdala was more strongly correlated with LBAS in the anterior olfactory nucleus than with that in the OB periphery. LBAS did not correlate with systemic tauopathy or amyloid β amyloidosis. These results indicate a high incidence of LBAS in the aging human OB; they also suggest that LBAS extends from the periphery to the anterior olfactory nucleus and results in clinical manifestations of LB disease.

Key Words: α-Synuclein, Anterior olfactory nucleus, Dementia with Lewy bodies, Incidental Lewy bodies, Olfactory bulb, Parkinson disease.

From the Department of Neuropathology (RS, YS, MI, HH, YS, SM), Tokyo Metropolitan Institute of Gerontology; Department of Neurology (RS, KI), The Jikei University School of Medicine; Departments of Pathology (YS, TA, MS) and Neurology (KK), Tokyo Metropolitan Geriatric Hospital, Tokyo, Japan; Department of Biostatistics (NT), Harvard School of Public Health, Boston, Massachusetts; and Department of Neurology (HM), Juntendo University, Tokyo, Japan.

Send correspondence and reprint requests to: Shigeo Murayama, MD, PhD, Department of Neuropathology, Tokyo Metropolitan Institute of Gerontology, 35-2 Sakaecho, Itabashi-ku, Tokyo 173-0015, Japan; E-mail: smurayam@tmig.or.jp

This study was supported by the Aid for Scientific Research Basic B (S.M. and Y.S.), Basic C (Y.S.), and Priority Areas (Advanced Brain Science Project) (S.M. and Y.S.) from the Ministry of Education, Culture, Sports, Science, and Technology of Japan.

INTRODUCTION

Olfaction is a major target of neuroscience research, and numerous genes are expressed for olfactory receptors (1,000 in mouse and 300 in human) (1–3). Patients with schizophrenia exhibit olfactory dysfunction (4–7) and loss of volume of the olfactory bulb (OB) (8). Olfactory dysfunction is also an early sign of Alzheimer disease (AD) and Lewy body (LB) diseases (i.e. Parkinson disease [PD], PD with dementia [PDD], and dementia with LB [DLB]) (9–19) and has been used to differentiate these disorders from progressive supranuclear palsy (20). Atrophy of the OB as revealed by magnetic resonance imaging has been reported to be useful diagnostic tools for AD (21) and PD (22). Recently, neuroprogenitor cells that migrate from the subventricular zone were identified in the human OB (23). Twice as many tyrosine hydroxylase (TH)–immunoreactive neurons were reported in the OBs of PD patients compared with those of age- and sex-matched controls (24). Thus, it is of interest as to whether LB-related α-synucleinopathy (LBAS) involves the TH system in the OB.

Subsequent to the staging system for diffuse LB disease proposed by Kosaka (25), Braak et al (26) suggested a neuropathologic staging procedure for idiopathic PD in an aged cohort that included PDD patients but not DLB or other patients with dementia and LB pathology. The latter subgroup included the amygdala variant of LB disease (27) complicated by AD (28, 29) or other tauopathies (29). According to Braak et al, the LBAS in the central nervous system (CNS) first affects the medulla oblongata, rostrally extends to the locus coeruleus, and reaches the substantia nigra. Braak et al (30) also reported a pattern of extension from the OB to the amygdala, but neither Kosaka et al nor Braak et al (30) examined possible statistical correlations between these 2 patterns in the extension of LBAS.

In light of these previous studies, we began to include the OB in routine neuropathologic examinations and noticed that LBAS in the OB is dominant either in the anterior olfactory nucleus (AON) or in the peripheral OB. Among several anatomical nomenclature systems of OB (31–34), we adopted that of Price (34) as follows: The axons of the bipolar receptor cells (approximately 6 million per nose) in the olfactory epithelium (the primary olfactory structure) ramify in the most superficial layer of the OB, the olfactory nerve layer. They

then form synapses with the dendrites of the secondary olfactory structure that consists of mitral and tufted cells in the glomerular layer. The external plexiform layer contains the dendrites of the mitral cells and the somata of the tufted cells. The mitral cell layer is formed by the somata of the mitral cells. The axons of the mitral cells run through the internal plexiform layer and reach the granule cell layer (Fig. 1). These secondary olfactory structures are the major anatomical regions that exhibit LBAS in the OB periphery. The AON is located in the OB and olfactory peduncle; it includes several groups of pyramidal-like cells and is termed tertiary olfactory structures.

The goal of this study was to clarify the significance of LBAS involving the OB in human aging. The OB periphery (including axon terminals of the primary structure and the soma, dendrites, and axons of the secondary structure) and AON (the axon terminals of the secondary structure and the soma, dendrites, and axons of the tertiary structure) were evaluated separately to study the extension pattern of LBAS.

MATERIALS AND METHODS

Tissue Source

Tissue samples were collected at the Tokyo Metropolitan Geriatric Hospital, which, as previously reported (29), provides community-based medical service to the aged population. Between 2003 and 2006, 320 consecutive autopsy brains, spinal cords, and adrenal glands (29) from 180 men and 140 women were used for this study. Two hundred forty-seven of the 320 cases overlapped with our recent studies of LB pathology in the skin (35). The patients' age ranged from 52 to 104 years old, with a mean ± SD age of 81.5 ± 8.5 years. The postmortem interval ranged from 52 to 4,210 minutes, with a mean of 753 minutes.

Neuropathology

Brains and spinal cords were examined as reported previously (36). In brief, 1 hemisphere was preserved for biochemical and molecular studies, and the other portions were prepared for morphological studies. After fixation in formalin, the representative areas were embedded in paraffin. Serial 6-μm-thick sections were stained with hematoxylin and eosin (H&E) and Klüver-Barrera methods. Selected sections were further examined with modified methenamine (37) and Gallyas-Braak silver (38) staining for senile changes, Congo red for amyloid deposition, and elastica Masson trichrome stain for vascular changes.

Immunohistochemistry

Selected sections were immunostained using a Ventana 20NX autostainer (Ventana, Tucson, AZ), as previously

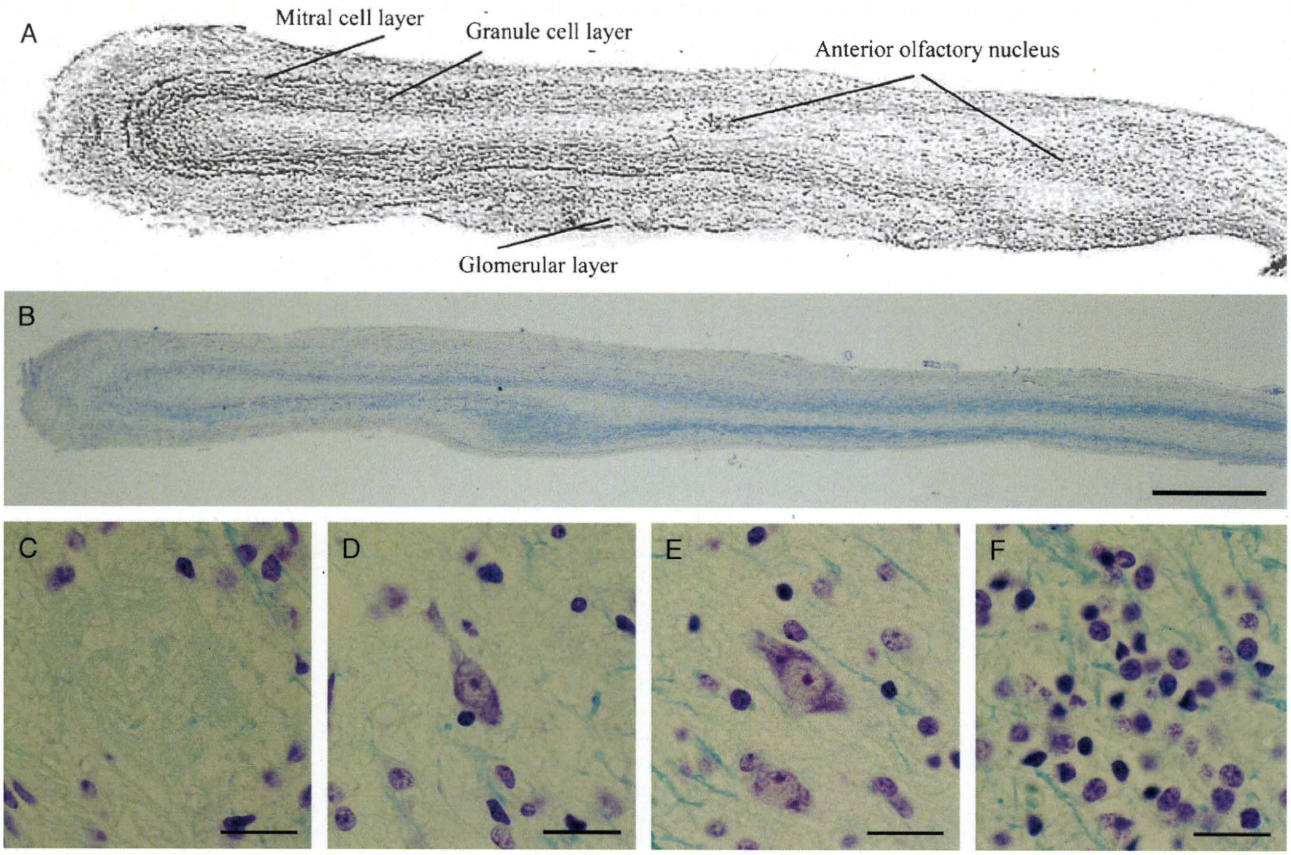

FIGURE 1. Schema and pathology of a sagittal section of the human olfactory bulb (OB). **(A)** Schema of the sagittal section of the human OB. Reproduced with permission from Elsevier © 2008 (34). **(B)** A representative sagittal section of the human OB. Scale bar = 1 mm. **(C)** Olfactory glomerulus. Scale bar = 25 μm. **(D)** Tufted cell. Scale bar = 25 μm. **(E)** Mitral cell. Scale bar = 25 μm. **(F)** Granule cell layer. Scale bar = 25 μm. **(B–F)** Klüver-Barrera method staining.

described (36). We immunostained representative sections as well as OBs from all patients with anti-phosphorylated α-synuclein (psyn; monoclonal, psyn no. 64 [39] and polyclonal PSer129 [40]), anti-phosphorylated tau (ptau; AT8, monoclonal; Innogenetics, Temse, Belgium), anti-β amyloid 11-28 (12B2, monoclonal; IBL, Maebashi, Japan), anti-ubiquitin (polyclonal, DAKO, Glostrup, Denmark), and anti-TH (monoclonal; Calbiochem-Novabiochem Corp, Darmstadt, Germany, and ImmunoStar, Hudson, WI) antibodies.

Evaluation of LBAS

To evaluate LBAS, we used immunohistochemistry with anti-psyn antibodies to screen OB sections, bilateral adrenal glands, medulla oblongata at the level of the dorsal motor nucleus of the vagus, upper pons at the level of the locus coeruleus, midbrain, amygdala, and posterior hippocampus. If anti-psyn immunoreactivity was observed in any of these regions, further studies with anti-psyn and ubiquitin antibodies were conducted on the anatomical structures as recommended by the original and revised DLB Consensus Guidelines (41, 42), PD staging by Braak et al (26), and our own previous work (39), which includes staining of CA2 of the hippocampus and intermediolateral column of the thoracic spinal cord (43), for staging of LBAS (42, 44). Our revised LB staging system (29) was applied to all patients as follows: Stage 0, no anti-psyn immunoreactive structure; Stage 0.5, Lewy dots or neurites only or fine granular cytoplasmic staining without any focal aggregates; Stage I, a few LBs confirmed by H&E staining, without neuronal loss (incidental LB disease); Stage II, abundant LBs with loss of pigmentation in the substantia nigra but without attributable parkinsonism or dementia (subclinical LB disease); Stage III, PD without dementia; Stage IV, DLB or PDD, transitional (limbic) form (DLBT or PDDT); and Stage V, DLB or PDD, neocortical (diffuse) form (DLBN or PDDN). Parkinson disease with dementia was differentiated from DLB by applying the "12-month" rule noted in the Consensus Guidelines (i.e. "dementia appears more than 1 year after the onset of parkinsonism") (41, 42). We subcategorized our Stage II patients into brainstem (B), transitional or limbic (T), and neocortical (N) forms based on Lewy score (41) and involvement of the intermediolateral column of the spinal cord (43) or the amygdala variant (A), as previously reported (27, 28). Stage 0.5 and Stage 1 patients were also subcategorized to the extent of LBAS localized in the brainstem (B), spreading to the limbic system (T) and neocortex (N) or preferentially present in amygdala (A), as previously reported.

Evaluation of Other Senile Changes and Neuropathologic Diagnosis

Neurofibrillary tangles (NFTs) were classified into Braak and Braak's (45) 7 stages (0–VI) and senile plaques (SPs) into 4 stages (0–C). Argyrophilic grains were classified into our 4 stages (0–III), as reported previously (46). The

TABLE 1. LBAS in the CNS and OB

BBAR LB Stage*	No.	LBAS in the OB	OB LBAS Grade								
			Periphery				AON				
			0	1	2	3	0	1	2	3	4
0	218	0	218	0	0	0	218	0	0	0	0
0.5	30	17	15	10	3	2	21	7	1	1	0
0.5B	8	3	5	2	0	1	7	0	0	1	0
0.5T	8	5	3	3	1	1	5	2	1	0	0
0.5A	14	9	7	5	2	0	9	5	0	0	0
I	37	33	4	4	17	12	10	10	9	5	3
IB	16	13	***3***	***2***	***7***	***4***	***7***	***7***	***1***	***1***	***0***†
IT	14	13	***1***	***1***	***8***	***4***	***1***	***3***	***4***	***3***	***3***
IA	7	7	***0***	***1***	***2***	***4***	***2***	***0***	***4***	***1***	***0***
II	8	8	0	1	4	3	0	2	1	3	2
IIB	3	3	0	0	3	0	0	1	0	2	0
IIT	4	4	0	1	1	2	0	1	1	1	1
IIA	1	1	0	0	0	1	0	0	0	0	1
III	2	2	0	2	0	0	0	0	1	0	1
IIIT	1	1	0	1	0	0	0	0	0	0	1
IIIN	1	1	0	1	0	0	0	0	1	0	0
IV	11	11	0	2	7	2	**0**	**0**	**4**	**5**	**2**†
V	14	14	0	2	10	2	**0**	**0**	**1**	**2**	**11**
Total	320	85	237	21	41	21	249	19	17	16	19

Correlation between OB periphery and AON grade in BBAR LB Stages IB, IT, and IA (bold and italic group).
p values are 0.006, 0.754, and 0.125, respectively.
Correlation between BBAR LB Stages IV and V (bold group), p = 0.005.
*BBAR LB stage (29, 39, 44).
†, p < 0.01.
A, amygdala variant; AON, anterior olfactory nucleus; B, brainstem; BBAR, Brain Bank for Aging Research; LB, Lewy body; LBAS, LB-related α-synucleinopathy; N, neocortical; OB, olfactory bulb; T, transitional.

neuropathologic diagnosis of AD was based on our definition (47), which proposes a modification of the National Institute on Aging and Reagan Institute criteria (48). The diagnoses of dementia with grains and NFT-predominant forms of dementia were based on the definitions of Jellinger (49) and Jellinger and Bancher (50). The diagnosis of progressive supranuclear palsy was based on the National Institute of Neurological Disorders and Stroke criteria (51). The diagnosis of vascular dementia was based on the criteria of the National Institute of Neurological Disorders and Stroke-Association Internationale pour la Recherche et l'Enseignement en Neurosciences (52). With respect to combined pathologies, the diagnosis of AD plus DLB was based on Braak NFT Stage equal to or more than IV and SP Stage C (47), in combination with a Lewy score equal to or more than 4 with involvement of the CA2 of hippocampus and intermediolateral column of the spinal cord, as previously reported (29, 43).

Neuropathology of the OB

Both OBs were sampled at autopsy. One was snap frozen, and the other was fixed in 4% paraformaldehyde for 48 hours. A sagittal section was embedded in paraffin, and 6-μm-thick serial sections were stained with H&E, with Klüver-Barrera, or by immunohistochemistry with the same panel of antibodies previously described.

In addition, a double labeling immunofluorescence study was performed on selected sections of the OB. Deparaffinized sections were incubated simultaneously with polyclonal psyn (PSer129) and monoclonal anti-TH or polyclonal ptau (AP422, polyclonal, a gift from Dr Y. Ihara) (53) and monoclonal psyn no. 64. Primary antibodies were visualized with anti-rabbit Alexa 546 Fluor and anti-mouse immunoglobulin G Alexa 488 (Molecular Probes, Eugene, OR) with 4′,6-diamidino-2-phenylindole (DAPI) staining for the nucleus under a confocal laser microscope (LSM5, PASCAL, Carl Zeiss, Jena, Germany).

LB Grade of the OBs

The OB periphery and the AON (Fig. 1) were separately evaluated. The secondary olfactory structure included the soma and cell processes of mitral cells, tufted cells, granule cells, and periglomerular cells. Grading of α-synuclein pathology followed the revised DLB Consensus

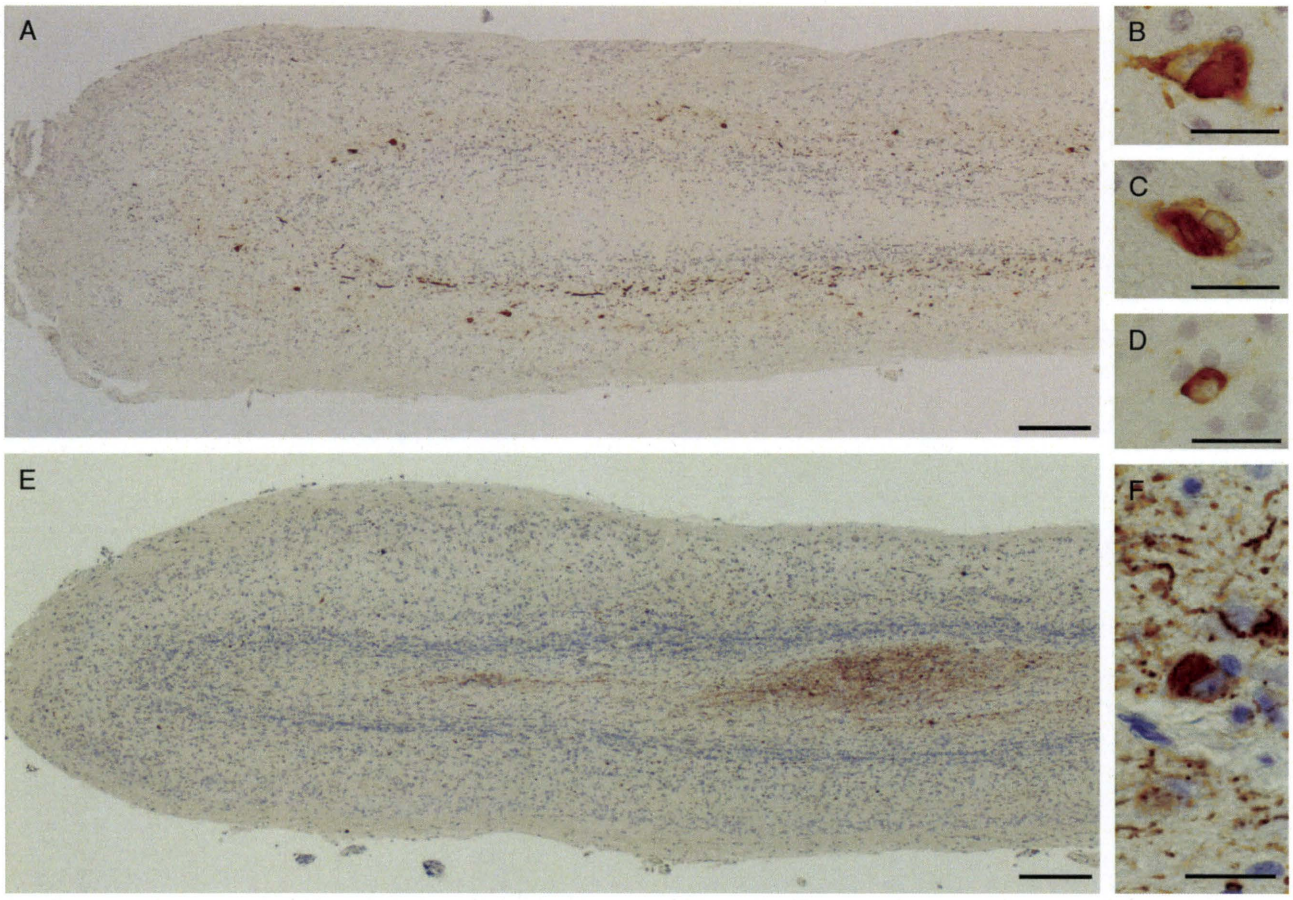

FIGURE 2. Lewy body (LB)–related α-synucleinopathy (LBAS) in different neuron populations in the olfactory bulb (OB). **(A)** Tissue from a patient with LBAS preferentially involving the periphery of the OB and surrounds the anterior olfactory nucleus (AON). Scale bar = 500 μm. **(B)** Mitral cell. Scale bar = 10 μm. **(C)** Tufted cell. Scale bar = 10 μm. **(D)** Granule cell. Scale bar = 10 μm. **(E)** Tissue from a patient with LBAS preferentially involving the AON. Scale bar = 500 μm. **(F)** AON neuron. Scale bar = 10 μm. **(A–F)** Immunohistochemistry with anti-phosphorylated α-synuclein antibody (psyn no. 64) counterstained with hematoxylin.

TABLE 2. Correlation Between LBAS Grades in the AON and in the Periphery of the OB

		LBAS Grade: AON		
		0	1	2≦
LBAS grade: Periphery	0	235	2*	0
	1	10	4	7
	2≦	4	13	45

$p = 0.004$.
*, complicated by coexistent Alzheimer disease pathology.
AON, anterior olfactory nucleus; LB, Lewy body; LBAS, LB-related α-synucleinopathy; OB, olfactory bulb.

TABLE 3. Correlations Between LBAS Grades in the AON and the OB Periphery With Clinical and Subclinical LB Disease

LBAS Grade	Periphery			
AON	0	1	2	3
0	0/0	0/10	0/2	0/2
1	0/2	0/4	0/10	0/3
2	0/0	1/2	3/7	1/8
3	0/0	2/2	5/11	0/3
4	0/0	3/3	9/11	2/5

The ratio represents the number of patients with clinical LB disease/the number of patients with either subclinical or clinical LB disease for each LBAS grade as described in the Materials and Methods section.
AON, anterior olfactory nucleus; LB, Lewy body; LBAS, LB-related α-synucleinopathy.

Guidelines (42). The classification of Tsuboi et al (54) for NFTs was applied. For SPs, we developed the following criteria: Grade 0, none; Grade 1, sparse dots; Grade 2, definite SPs, scattered; and Grade 3, abundant SPs.

Clinical Information

Clinical information, including the presence or absence of parkinsonism and cognitive state, was obtained from medical charts. The Mini-Mental State Examination (55) or the Hasegawa Dementia Scale (or its revised version [56]), and the Instrumental Activities of Daily Living (57) were used to evaluate cognitive function. The Clinical Dementia Rating (CDR) (58) was retrospectively determined by 2 independent board-certified neurologists. If the resulting ratings were in agreement, the score was accepted. If not, the neurologists reconciled their differences in the score after interviews with the patients' attending physicians and caregivers. Information about parkinsonism, bradykinesia, resting tremor, rigidity, and postural instability was obtained from neurological examinations. The presence of more than 2 of these clinical signs was interpreted as indicative of parkinsonism. The clinical diagnosis of AD was based on the criteria of the National Institute of Neurological and Communication Disorders and Stroke–Alzheimer Disease and Related Disorders Association (59).

Apolipoprotein E Genotype Analysis

We extracted genomic DNA from a freshly frozen kidney, measured the quantity of DNA with a spectrophotometer (Hitachi U2000, Tokyo, Japan), and adjusted it to 100 μg/mL. Tissues from all patients except for one (who had Creutzfeldt-Jakob disease) in the series were genetically examined in our laboratory. After polymerase chain reaction amplification, apolipoprotein E (APOE) genotyping was conducted with restriction enzyme *Hha*I, as described previously by Hixson and Vernier (60).

Statistical Analysis

Statistical comparison of LBAS grades in the AON and the OB periphery among patients at the Brain Bank for Aging Research (BBAR) (61) LB Stages IB, IT, IN, and IA (I, incidental LB disease; with extension of B, brainstem; T, transitional; N, neocortical; and A, amygdala as previously stated) was performed by the Friedman test. The Friedman test was used for comparison of categorical data. The Mann-Whitney U test was used for comparison of age at death. The relationships between LBAS grade in the OB and LBAS in the adrenal gland were assessed with the Mann-Whitney U test. Independent-sample *t*-tests were used for comparison of mean LBAS grade in the AON or the OB periphery and between Braak stages for SP and NFTs and the BBAR LB stage. The correlation between LBAS grade of the amygdala and of the AON or the OB periphery was assessed with Spearman rank correlation coefficient. Statistical comparison of LBAS grades, tau grades, and β-amyloid grades in AON and the periphery between APOE ε4 carriers and noncarriers using the Wilcoxon test. All statistical analyses were

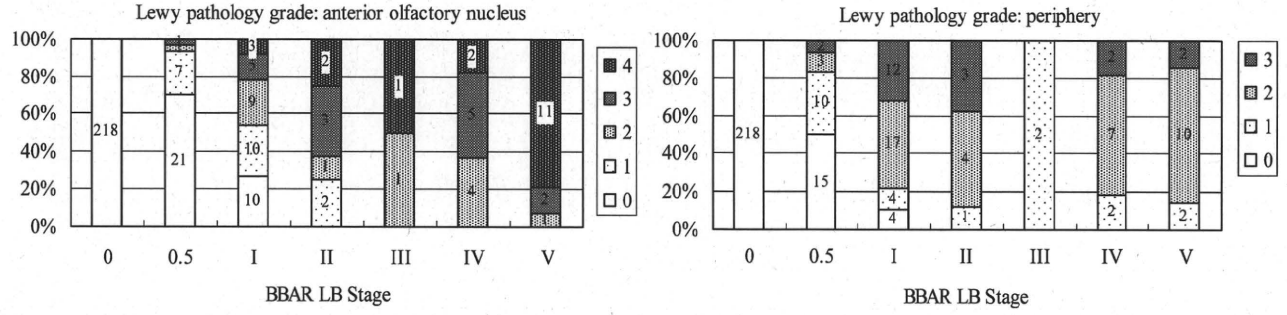

FIGURE 3. Correlations between Lewy body (LB) stage of the Brain Bank for Aging Research (BBAR) and grade of LB-related α-synucleinopathy (LBAS) in the anterior olfactory nucleus or the periphery of the olfactory bulb (OB). All patients with BBAR LB Stage ≥ II had LBAS in the OB.

TABLE 4. Correlations Between LBAS Grades in the OB and Degenerative Senile Changes in Other Areas of the CNS

	BBAR LB Stage			Braak SP Stage			Braak NFT Stage		
LBAS Grade	**0.5–II**	**III–V**	**p**	**0–A**	**B–C**	**p**	**0–II**	**III–VI**	**p**
AON	1.53	3.35	<0.001	1.76	2.33	0.051	2.05	2.12	0.814
Periphery	1.98	1.88	0.538	1.92	1.98	0.719	1.93	1.98	0.786

AON, anterior olfactory nucleus; BBAR, Brain Bank for Aging Research; LB, Lewy body (0.5–II, subclinical LB disease; III–V, Parkinson disease, Parkinson disease with dementia, and dementia with LBs); LBAS, LB-related α-synucleinopathy; NFT, neurofibrillary tangle; OB, olfactory bulb; SP, senile plaque.

performed using SPSS 15.0J for Windows (SPSS, Inc, Chicago, IL). The statistical significance level was set at $p < 0.05$.

RESULTS

Clinical Information

Among the 320 consecutive autopsy patients, 47 fit clinical criteria for parkinsonism (41). The CDR could retrospectively be assessed in 251 patients as follows: CDR 0, 95 patients; CDR 0.5, 41 patients; CDR 1, 31 patients; CDR 2, 15 patients; and CDR 3, 69 patients. The percentage of CDR equal to or greater than 0.5 was 62.2%.

Neuropathologic Diagnosis

The neuropathologic diagnoses consisted of AD (n = 25), vascular dementia (n = 20), DLB (n = 13), dementia with grains (n = 10), progressive supranuclear palsy (n = 6), PDD (n = 5), NFT-predominant form of dementia (n = 5), amyotrophic lateral sclerosis (n = 5), amyotrophic lateral sclerosis with dementia (n = 5), idiopathic hippocampal sclerosis (n = 3), PD (n = 2), and 1 case each of PD with Pick bodies, spinocerebellar ataxia 3/Machado-Joseph disease, multiple sclerosis, Kennedy-Alter Sung disease, Huntington disease, frontotemporal lobar degeneration with ubiquitinated inclusions, and Creutzfeldt-Jakob disease. Patients with combined pathologies included AD plus DLB (n = 6), AD plus vascular dementia (n = 2), dementia with grains plus NFT-predominant form of dementia (n = 2), and PDD plus progressive supranuclear palsy plus dementia with grains (n = 1). The remaining patients did not fulfill clinical and/or pathological criteria for neurodegenerative diseases.

The BBAR Staging for LBAS in the CNS, Including Spinal Cord

Lewy body–related α-synucleinopathy was found in 102 (31.9%) of the 320 patients (Table 1); the BBAR LB stages (29, 39, 44) were as follows: Stage 0, 218 patients; Stage 0.5, 30 patients; Stage I, 37 patients; Stage II, 8 patients; Stage III, 2 patients; Stage IV, 11 patients; and Stage V, 14 patients. The Stage IV patients included 4 of PDDT and 7 of DLBT, with 5 of the 7 DLBT patients having parkinsonism. The Stage V patients included 2 with PDDN and 12 with DLBN; 3 of the 12 DLBN patients had parkinsonism (42).

Incidence, Distribution, and Extent of LBAS in the OB

Lewy body–related α-synucleinopathy was detected in the OB of 85 (26.6%) of the 320 patients. The most frequent psyn-immunoreactive neuronal cells in the periphery were granule cells, followed by mitral cells, tufted cells, and periglomerular cells (Fig. 2). Lewy bodies in the OBs usually showed cortical-type morphological features, as reported previously (11); a few had halos.

Patients with LBAS in the OBs could be classified into 2 groups: one in which LBAS predominated in the AON (Fig. 2E) and the other in which LBAS predominated in the periphery of the OB (Fig. 2A). Very few psyn-positive neurites or dots were present in the olfactory nerve layer (where ramified axons of the bipolar receptor cells are present in the olfactory epithelium); therefore, LBAS in the periphery was found to reside mainly in the secondary olfactory structure. Lewy body–related α-synucleinopathy in

TABLE 5. Demography of 5 Patients With LB Identified Only in the OBs by H&E Stain

									LBAS								
								BBAR LB	OB Grade		Other Regions						
Patient	**Age/Sex**	**Clinical Dx**	**CDR**	**BW, g**	**Np Dx**	**NFT**	**SP**	**Stage**	**AON**	**Periphery**	**dm**	**lc**	**sn**	**a**	**ca2**	**sc**	**adr**
1	72/M	HCC	0.5	1351	unremarkable	I	A	0.5T	1	2	0	1	1	1	1	0	0
2	78/F	CRF dementia	2	1147	CVDE, VD	II	A	0.5B	3	3	1	1	1	1	0	0	0
3	89/M	Lung carcinoma post radiation therapy	1	1246	early AD	IV	C	0.5A	2	2	0	0	0	1	0	1	0
4	74/M	COPD	0.5	1413	AC	V	C	0.5T	2	3	1	1	1	1	1	0	0
5	82/F	AD	3	1123	AD	V	C	0.5A	1	2	0	0	0	1	0	0	0

a, amygdala; AC, Alzheimer disease changes; AD, Alzheimer disease; adr, adrenal gland; AON, anterior olfactory nucleus; BBAR, the Brain Bank for Aging Research; BW, brain weight; ca2, ca2 of the hippocampus; CDR, clinical dementia rating; COPD, chronic obstructive pulmonary disease; CRF, chronic renal failure; CVDE, clinically significant embolic cerebral vascular disease; dm, dorsal motor nucleus of vagus; Dx, diagnosis; F, female; H-E, hematoxylin and eosin; HCC, hepatic cell carcinoma; LB, Lewy body; LBAS, LB-related α-synucleinopathy; lc, locus caeruleus; M, male; NFT, Braak's stages for neurofibrillary tangles; Np, neuropathologic; OB, olfactory bulb; sc, spinal cord; sn, substantia nigra; SP, Braak's stages for senile plaques; VD, vascular dementia.

the AON was graded from 0 to 4 and LBAS in the OB periphery from 0 to 3. The AON Grades 3 and 4 patients were combined and analyzed with the Periphery Grade 3 patients.

Among the patients with LBAS in the OB, 14 were affected in the periphery alone and 2 in the AON alone. The latter 2 patients had AD and had very few psyn-immunoreactive granules in neuronal perikarya. In the earliest stage of LBAS in the OB, the periphery was more frequently involved than the AON (Table 2; $p = 0.004$).

Correlations Between LBAS in the OB and the CNS, Including Spinal Cord

Lewy body–related α-synucleinopathy in the OB was compared with LBAS in other locations of the CNS (Table 1; Fig. 3). The percentages of OB LBAS–positive patients at each BBAR LB stage were as follows: Stage 0, 0%; Stage 0.5, 56.7% (0.5B, 37.5%; 0.5T, 62.5%; 0.5A, 64.3%); Stage I, 89.2% (IB, 81.3%; IT, 92.9%; IA, 100%); and Stages II to V, 100% (Table 1; Fig. 3).

Among the 35 patients at BBAR LB Stage II or higher, 31 (88.6%) had LBAS in the adrenal glands. The 4 patients who lacked adrenal LBAS all had AD pathology. The average LBAS grade in the OB periphery of the 31 adrenal LBAS–positive patients was significantly greater ($p = 0.029$) than that of the 4 adrenal LBAS–negative patients. In contrast, the average LB grade in the AON of the 4 adrenal LBAS–negative patients was greater than that of the 31 adrenal LBAS–positive patients, although the difference was not significant ($p = 0.054$).

We further analyzed patients categorized as having BBAR LB Stage I. In the IB subgroup, the average LBAS grade of the periphery was significantly larger ($p < 0.01$) than that of the AON, but this difference was not significant in the IT and the IA subgroups ($p = 0.75$, $p = 0.13$; Table 1).

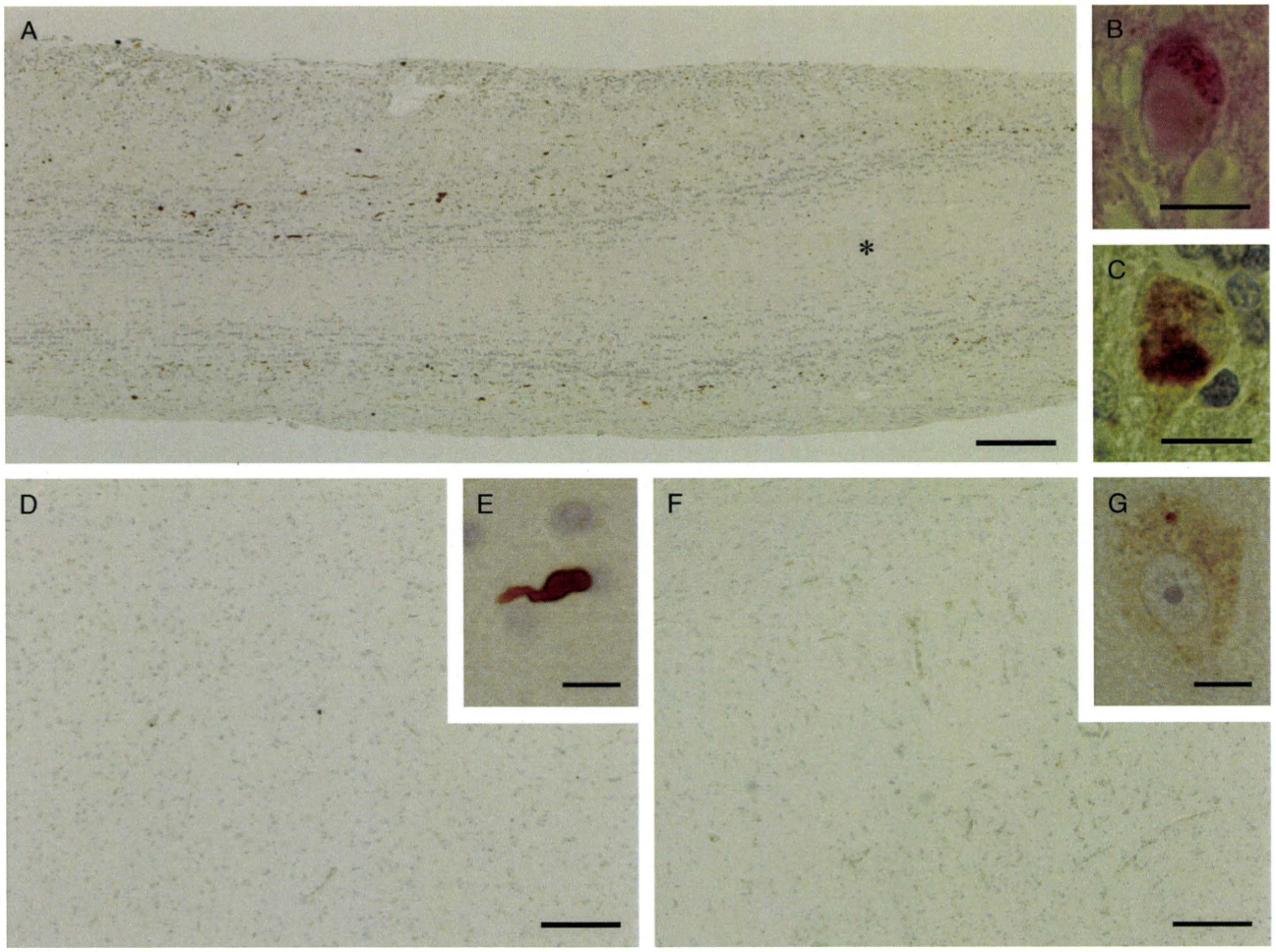

FIGURE 4. Tissue from a patient with Lewy bodies (LBs) only in the olfactory bulb (OB) (Patient 1 in Table 5). **(A)** LB-related α-synucleinopathy in the periphery of the OB (*anterior olfactory nucleus; immunohistochemistry (IH) with anti-phosphorylated α-synuclein antibody, visualized with diaminobenzidine. Scale bar = 200 μm. **(B)** LB in the periphery of the OB (H&E stain). Scale bar = 10 μm. **(C)** Intraneuronal perikaryal aggregates are stained by IH with anti-phosphorylated α-synuclein antibody (psyn no. 64). Scale bar = 10 μm. **(D)** IH with psyn no. 64 in the amygdala. Scale bar = 200 μm. **(E)** A single Lewy neurite is stained. Scale bar = 10 μm. **(F)** CA2 in the hippocampus shows almost no IH staining with psyn no. 64. Scale bar = 200 μm. **(G)** A fine granule is psyn no. 64 immunopositive in a neuron perikaryon. Scale bar = 10 μm.

All of the patients at BBAR LB Stage III or higher (PD/PDD/DLB) demonstrated high-grade LBAS in the AON. The mean grade of LBAS in the AON among patients at Stage V was significantly higher than that of Stage IV patients ($p = 0.005$; Table 1). One of 11 Stage IV patients and 5 of 14 Stage V patients fulfilled our pathological criteria of AD (47), and all of them (6/6, 100%) showed LBAS Grade 4 in the AON. In contrast, only 7 (36.8%) of 19 patients at Stages IV and V who did not fulfill our pathological criteria for AD showed LBAS Grade 4 in the AON.

We also compared patients with subclinical (≤Stage II) and clinical (≥Stage III) LB disease with regard to LBAS grade of the AON and the periphery of the OB (Table 3). The average LBAS grade in the AON, but not in the periphery, was significantly higher in clinical than in subclinical patients (Table 4).

LBAS in Amygdala and OB

Ninety-four (29.4%) of the 320 patients had LBAS in the amygdala. Among the 85 patients with positive LBAS in the OB, 83 had LBAS in the amygdala; the remaining 2 had Grade 1 LBAS in the periphery of the OB but not in the AON or amygdala. Five had Grade 1 LBAS in the amygdala but LBs in the OB (see later). All of the PD/PDD/DLB (BBAR LB Stages III, IV, and V) patients had Grade 4 LBAS in the amygdala, in accordance with the grading paradigm of the revised DLB Consensus Guidelines (42). The LBAS grade of the amygdala correlated more strongly with that of the AON than with that of the OB periphery (Spearman correlation coefficient, 0.853 and 0.521, respectively).

Correlations Between Braak's Stages for NFTs or SPs and LBAS in the OB

The mean LBAS grade of the AON was higher in Braak's SP Stages B and C than in Stages 0 and A ($p = 0.051$), although this difference was not statistically significant. Comparisons of other Braak stages did not reveal any statistical differences (Table 4).

Influence of APOE ε4 on Olfactory LBAS

The results of APOE genotyping of the 319 patients (excluding one with Creutzfeldt-Jakob disease) were as follows: 2 patients with the ε2/ε2 genotype; 12 with ε2/ε3; 1 with ε2/ε4; 247 with ε3/ε3; 51 with ε3/ε4; and 6 with ε4/ε4. The 57 APOE ε4 carriers had a significantly higher grade than the 262 noncarriers for tauopathy of the AON ($p = 0.011$) and anti-β amyloid amyloidosis of both the AON ($p < 0.001$) and the periphery ($p = 0.001$), but not for LBAS of the AON ($p = 0.80$) or the periphery ($p = 0.28$).

Correlation Between Incidence of LBAS of the OB and Age at Death

The mean age at death was 84.1 ± 8.1 years in OB-positive patients and 80.6 ± 8.6 years in OB-negative patients ($p = 0.014$). Although not statistically significant, the percentage of LBAS in the OB among those patients with LBAS involving the CNS also tended to increase with age: 73% (22/30) in the eighth decade, 87% (34/39) in the ninth decade, and 93% (25/27) in the 10th decade. No significant difference was noted between OB-positive and OB-negative patients with respect to sex.

Analysis of Data on the 5 Patients Who Had LBs Only in the OB by Routine H&E Stain

Among the 320 consecutive autopsy patients, 5 (1.6%) who were categorized as having BBAR LB Stage 0.5 had LBs recognized by H&E staining only in the OB (Table 5). No adrenal LBAS was found in these 5 patients. The group consisted of 3 men and 2 women, with a mean age at death of 79 years. One patient (Patient 1) had pure LBAS not markedly complicated by other senile changes or vascular

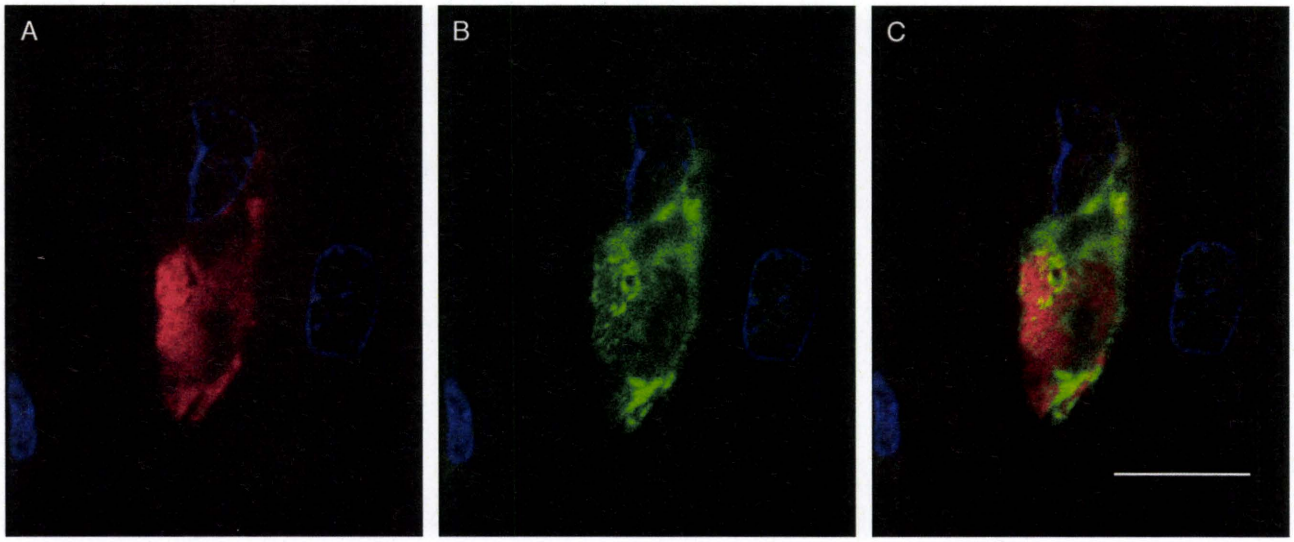

FIGURE 5. Colocalization of phosphorylated α-synuclein and tau in a neuron of the anterior olfactory nucleus visualized by confocal microscopy. There is little overlap in the staining. Patient 3 in Table 5. Scale bar = 10 μm. **(A)** Epitope of AP422 visualized with Alexa 546 Fluor (red). **(B)** Epitope of psyn no. 64, visualized with Alexa 488 Fluor (green). **(C)** Merged image. Nuclear stain with 4′,6-diamidino-2-phenylindole (DAPI) (blue).

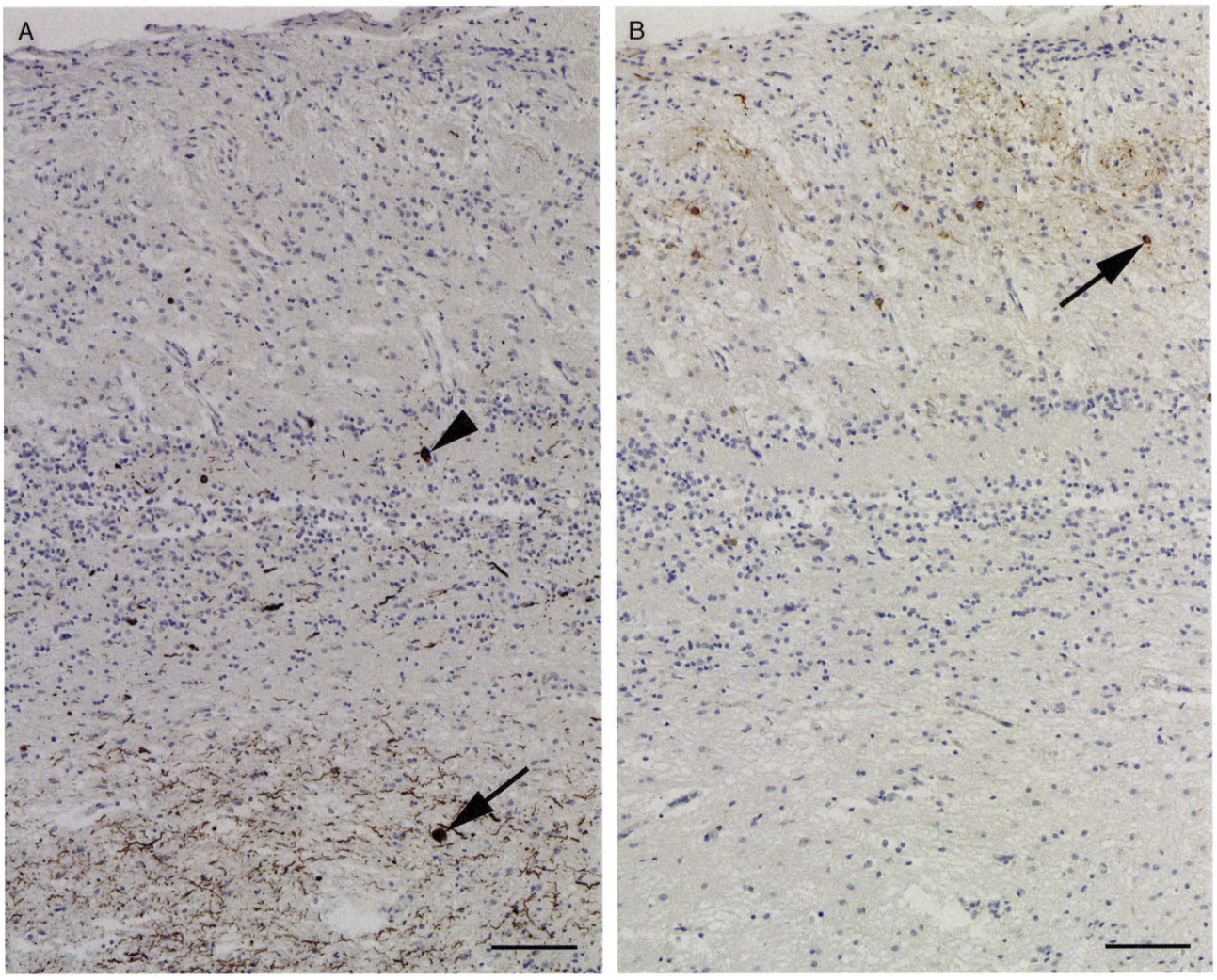

FIGURE 6. Different distribution patterns of the epitope of tyrosine hydroxylase (TH) and phosphorylated α-synuclein immunohistochemistry. **(A)** The epitope of anti-phosphorylated α-synuclein antibody was largely localized to mitral cells (arrowhead) and the granular cell layer and the anterior olfactory nucleus (arrow). Scale bar = 100 μm. **(B)** The epitopes of anti-TH antibodies were situated in periglomerular cells (arrow) and glomerulus.

lesions. Lewy body–related α-synucleinopathy preferentially involved the periphery of the OB (Fig. 4A), with a significant number of LBs (Figs. 4B, C). There were only a few anti-psyn–immunoreactive dots in the AON (Fig. 4A). Anti-psyn immunoreactivity was also present (but sparse) in the locus coeruleus, substantia nigra, amygdala (Figs. 4D, E), and CA2 of the hippocampus (Figs. 4F, G). Three of these patients had AD pathology, and all had colocalization of the epitopes of anti-psyn and ptau antibodies in neurons of the AON (Figs. 5A–C).

Correlation Between Anti-TH–Immunoreactive Neurons and LBAS

The epitopes of anti-TH antibodies were localized to periglomerular cells and very few granule cells in addition to the stratum album, as reported previously (62). The locations of the epitopes of anti-psyn antibodies were different from those of anti-TH antibodies and preferentially involved inner structures (Fig. 6). Very little colocalization of the epitopes of anti-psyn and TH antibodies could be detected (Figs. 7A–C).

DISCUSSION

There are 5 major findings in this study: 1) 26% of the consecutive autopsy patients from a general geriatric hospital had LBAS in the OB (peripheral OB, AON, or both); 2) LBAS always involved the OB in the advanced subclinical and clinical stages of LB disease; 3) in this aging population, LBs first appeared in the OB of 2% of patients; 4) LBAS in the OB appeared to extend from the periphery of the OB (secondary olfactory structure) to the AON (tertiary olfactory structure); and 5) LBAS in the amygdala was strongly correlated with LBAS in the OB; this correlation was more pronounced in the AON than in the periphery.

Subsequent to Kosaka et al (63), Braak et al (26) examined a cohort that consisted of incidental cases without

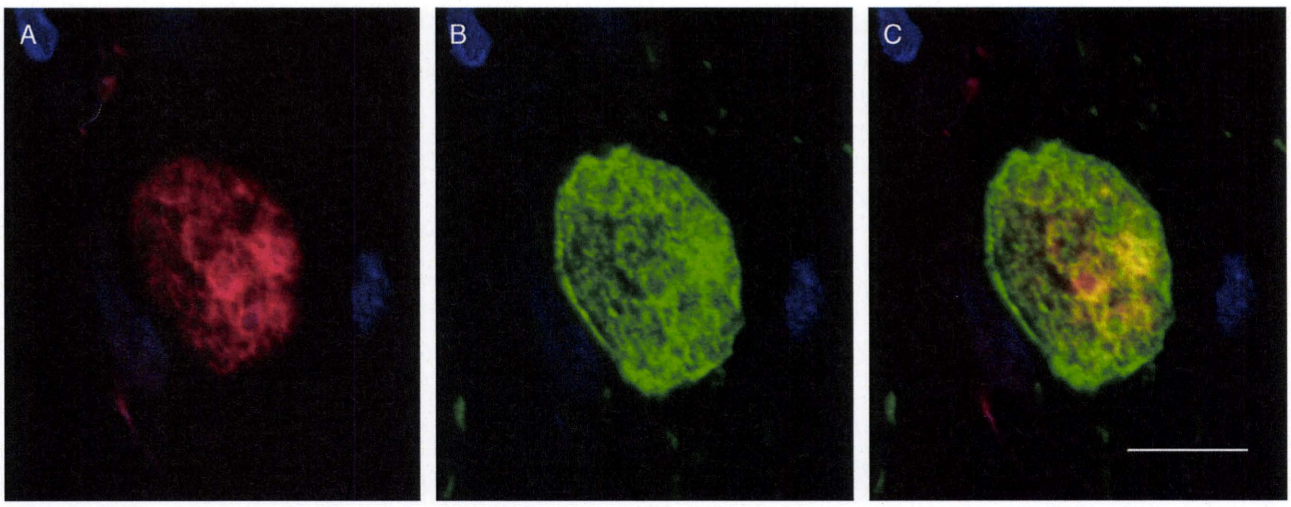

FIGURE 7. Epitopes of anti-phosphorylated α-synuclein antibody (PSer129) and anti–lltyrosine hydroxylase (TH) antibody were rarely colocalized. **(A)** Epitope of PSer129 visualized with Alexa 546 Fluor (red). Scale bar = 10 μm. **(B)** Epitope of TH visualized with Alexa 488 Fluor (green). **(C)** Merged image. Nuclear staining with 4′,6-diamidino-2-phenylindole (DAPI) (blue).

dementia and clinical PD patients with and without dementia, excluding AD and DLB by immunohistochemistry with anti–α-synuclein antibodies. They proposed a staging paradigm for LBAS, starting from the medulla oblongata, including the dorsal motor nucleus of the vagus, extending rostrally in the brainstem, spreading to the limbic system, and reaching the neocortex (26). Braak et al more recently reported findings in the OB and amygdala (30). The correlation between the Kosaka-Braak rostral extension pathway and the olfactory-amygdala pathway has yet to be determined. Three patients (Patients 1, 3, and 5 in Table 5) had LBAS in the OB but not in the dorsal motor nucleus of the vagus and did not follow the original staging of Braak et al (26). A difference between the study of Braak et al (30) and the present study is that although they evaluated both tertiary and secondary olfactory structures for the presence of LBAS, our examination of the various cell types and layers in the peripheral OB enabled us to conclude that the secondary olfactory structure is preferentially involved in early-stage LBAS.

Olfactory dysfunction is one of the initial manifestations in PD and occurs before motor dysfunction (64). An LB-type rapid eye movement sleep behavior disorder is also recognized to develop into PD, and a decrease in olfactory discrimination ability is also useful for the diagnosis of this disorder (65). We found that LBAS always involves the OB when LBAS includes degeneration of the substantia nigra, irrespective of the presence or absence of clinical parkinsonism or dementia; this suggests the morphological correlate of these clinical observations. Olfactory dysfunction is rarely recognized as a medical problem in the elderly in Japan, and we did not find descriptions of an impaired sense of smell in the retrospective investigation of medical charts.

Our findings that LBAS in the OB may start in the periphery and extend to the AON are in agreement with the results of Hubbard et al (66) who studied 79 OBs, 193 AON, and 201 amygdalae. Their specimens were independently registered in the Cambridge Brain Bank, and most of them had AD pathology. These studies may support the hypothesis of Hawkes et al (67) and Hawkes (68) that a neurotropic pathogen, probably viral, enters the brain through the olfactory pathway. Intranasal administration of the neurotoxin 1-methyl-4-phenyl-1,2,3,6-tetrahydropyridine to rats reduced the enzyme activity of TH in the OB and substantia nigra, resulting in a significant reduction in dopamine concentration in the OB and reproducing the clinical features of PD (69). In contrast, Huisman et al (24) reported that the total number of TH-immunoreactive neurons in the OB was twice as high in PD patients as in age- and sex-matched controls; they suggested that increased dopaminergic activity in the OB may lead to the suppression of olfactory information because of the inhibitory effect of dopamine on the transmission between olfactory receptor cells and mitral cells within the olfactory glomeruli (24). In the present study, the anatomical locations of LBAS and anti-TH–immunoreactive neurons rarely matched. The role of dopamine in olfactory dysfunction should, therefore, be further investigated to clarify these issues.

Our study also indicated a strong correlation between LBAS in the AON and LBAS in the amygdala. Three of 5 patients with LBs only in the OB also had AD pathology of NFT Stage IV or higher and we confirmed colocalization of the epitopes of anti-ptau and anti-psyn antibodies in the perikarya of AON neurons. Colocalization of these 2 epitopes has been reported in the amygdala, entorhinal cortex, and CA2 and 3 of hippocampus (70, 71), as well as in the OB (72). Fujishiro et al (72) first reported colocalization of α-synuclein and tau filaments in the OB with double enzyme immunocytochemistry and immunoelectron microscopy in the amygdala variant of LB disease complicated by AD. Because they screened AD patients with a considerable burden of LBAS in the amygdala and did not separately observe the changes in the periphery of the OB and AON, they could not determine in which direction(s) the LBAS spreads (Hiroki Fujishiro, the 49th Annual Meeting of the Japanese Society of Neuropathology, personal communication, Tokyo, May 2008). In contrast, Hubbard et al (66) proposed the

hypothesis that the spread of LBAS from the periphery of the OB to the AON and amygdala was independent. Taken together with these previous studies (66, 72), our present observations make it reasonable to conclude that in AD, LBAS first affects the periphery of the OB, spreads to the AON, and then reaches the amygdala. We also provide the first morphological evidence that the colocalization of tau and α-synuclein can first appear in the AON in AD with very little burden of α-synucleinopathy in the amygdala. Thus, we propose that the amygdala variant of LB disease should be renamed as the *olfactory-amygdala variant.*

The chief original observation of the present study is that we confirmed this pattern of spread in patients with pure Lewy pathology without AD. Moreover, our study clearly shows that the involvement of the periphery of the OB alone does not result in either Lewy body–associated parkinsonism or dementia. This suggests that the spread of LBAS in the AON and then into the amygdala may be required for the clinical manifestations of LB disease.

Our study also confirms the biologic significance of pale or LB seen in sections stained by H&E that corresponds to focal aggregates of immunoreactivity for phosphorylated α-synuclein. In the DLB revised Consensus Guidelines (42), which we followed, the presence of pale or LBs was determined to be equal to or more than Grade 2, whereas the presence of immunohistochemically visualized Lewy neurites or diffuse granular perikaryal neuronal staining alone, lacking pale or LBs, indicated Grade 1. Our results also indicate that the presence of LBs or pale bodies in AON (LBAS ≥ Grade 2) was correlated with a clinical presentation of LB disease (Table 3).

Thus, it is likely that the extension of LBAS from the OB periphery to the AON is essential for extension of LBAS from the OB to other areas of the CNS, including the amygdala. Recently, the presence of LBs in grafted fetal tissues in the striatum has been reported (73, 74), indicating the transmission of an LBAS pathogen through the neuronal network (67, 75, 76). Our present results are consistent with these new observations.

In conclusion, we show here that the OB is one of the initial anatomical sites affected by LBAS, and that its functional and morphological evaluation is useful for the neuropathologic diagnosis and clinical evaluation of LB disease.

ACKNOWLEDGMENTS

The authors thank Dr Takeshi Iwatsubo (Department of Neuropathology, University of Tokyo, Tokyo, Japan) and Dr Yasuo Ihara (Department of Neuropathology, Doshisha University, Kyoto, Japan) for the donation of antibody; Mr Naoo Aikyo, Mrs Mieko Harada, and Mrs Nobuko Naoi for the preparation of sections; and Dr Kinuko Suzuki for helpful discussions and comments. This study received the 2008 Moore Award at the annual meeting of the American Association for Neuropathologists, San Diego, CA, April 2008.

REFERENCES

1. Serizawa S, Ishii T, Nakatani H, et al. Mutually exclusive expression of odorant receptor transgenes. Nat Neurosci 2000;3:687–93
2. Buck L, Axel R. A novel multigene family may encode odorant receptors: A molecular basis for odor recognition. Cell 1991;65:175–87
3. Glusman G, Yanai I, Rubin I, et al. The complete human olfactory subgenome. Genome Res 2001;11:685–702
4. Bradley EA. Olfactory acuity to a pheromonal substance and psychotic illness. Biol Psychiatry 1984;19:899–905
5. Harrison PJ, Pearson RC. Olfaction and psychiatry. Br J Psychiatry 1989;155:822–28
6. Hurwitz T, Kopala L, Clark C, et al. Olfactory deficits in schizophrenia. Biol Psychiatry 1988;23:123–28
7. Moberg PJ, Agrin R, Gur RE, et al. Olfactory dysfunction in schizophrenia: A qualitative and quantitative review. Neuropsychopharmacology 1999;21:325–40
8. Turetsky BI, Moberg PJ, Yousem DM, et al. Reduced olfactory bulb volume in patients with schizophrenia. Am J Psychiatry 2000;157:828–30
9. Mesholam RI, Moberg PJ, Mahr RN, et al. Olfaction in neurodegenerative disease: A meta-analysis of olfactory functioning in Alzheimer's and Parkinson's diseases. Arch Neurol 1998;55:84–90
10. Daniel SE, Hawkes CH. Preliminary diagnosis of Parkinson's disease by olfactory bulb pathology. Lancet 1992;340:186
11. Hawkes CH, Shephard BC, Daniel SE. Olfactory dysfunction in Parkinson's disease. J Neurol Neurosurg Psychiatry 1997;62:436–46
12. Westervelt HJ, Stern RA, Tremont G. Odor identification deficits in diffuse Lewy body disease. Cogn Behav Neurol 2003;16:93–99
13. Sakuma K, Nakashima K, Takahashi K. Olfactory evoked potentials in Parkinson's disease, Alzheimer's disease and anosmic patients. Psychiatry Clin Neurosci 1996;50:35–40
14. ter Laak HJ, Renkawek K, van Workum FPA. The olfactory bulb in Alzheimer disease: A morphologic study of neuron loss, tangles, and senile plaques in relation to olfaction. In: *Alzheimer Disease and Associated Disorders*, vol. 8. New York, NY: Raven Press, 1994:38–48
15. Hawkes C. Olfaction in neurodegenerative disorder. Mov Disord 2003; 18:364–72
16. Ponsen MM, Stoffers D, Booij J, et al. Idiopathic hyposmia as a preclinical sign of Parkinson's disease. Ann Neurol 2004;56:173–81
17. Stiasny-Kolster K, Doerr Y, Moller JC, et al. Combination of "idiopathic" REM sleep behaviour disorder and olfactory dysfunction as possible indicator for alpha-synucleinopathy demonstrated by dopamine transporter FP-CIT-SPECT. Brain 2005;128:126–37
18. Ross GW, Abbott RD, Petrovitch H, et al. Association of olfactory dysfunction with incidental Lewy bodies. Mov Disord 2006;21:2062–67
19. Ross GW, Petrovitch H, Abbott RD, et al. Association of olfactory dysfunction with risk for future Parkinson's disease. Ann Neurol 2008; 63:167–73
20. Doty RL, Golbe LI, McKeown DA, et al. Olfactory testing differentiates between progressive supranuclear palsy and idiopathic Parkinson's disease. Neurology 1993;43:962–65
21. Thomann PA, Dos Santos V, Toro P, et al. Reduced olfactory bulb and tract volume in early Alzheimer's disease—a MRI study. Neurobiol Aging 2007 [Epub ahead of print]
22. Mueller A, Abolmaali ND, Hakimi AR, et al. Olfactory bulb volumes in patients with idiopathic Parkinson's disease a pilot study. J Neural Transm 2005;112:1363–70
23. Curtis MA, Kam M, Nannmark U, et al. Human neuroblasts migrate to the olfactory bulb via a lateral ventricular extension. Science 2007;315: 1243–49
24. Huisman E, Uylings HB, Hoogland PV. A 100% increase of dopaminergic cells in the olfactory bulb may explain hyposmia in Parkinson's disease. Mov Disord 2004;19:687–92
25. Kosaka K. Diffuse Lewy body disease in Japan. J Neurol 1990;237: 197–204
26. Braak H, Del Tredici K, Rub U, et al. Staging of brain pathology related to sporadic Parkinson's disease. Neurobiol Aging 2003;24:197–211
27. Hamilton RL. Lewy bodies in Alzheimer's disease: A neuropathological review of 145 cases using alpha-synuclein immunohistochemistry. Brain Pathol 2000;10:378–84
28. Uchikado H, Lin WL, DeLucia MW, et al. Alzheimer disease with amygdala Lewy bodies: A distinct form of alpha-synucleinopathy. J Neuropathol Exp Neurol 2006;65:685–97
29. Fumimura Y, Ikemura M, Saito Y, et al. Analysis of the adrenal gland is useful for evaluating pathology of the peripheral autonomic nervous system in lewy body disease. J Neuropathol Exp Neurol 2007;66:354–62

30. Braak H, Muller CM, Rub U, et al. Pathology associated with sporadic Parkinson's disease—where does it end? J Neural Transm 2006:89–97
31. Carpenter M. Olfactory pathways, hippocampal formation, and the amygdala. *Core Text of Neuroanatomy.* Baltimore, MD: Williams & Wilkins, 1991:361–89
32. Cleland TA, Lister C. Central olfactory structures. In: Doty R, ed. *Handbook of Olfaction and Gustation.* New York, NY: Marcel Dekker, 2003:165–80
33. Kovacs T. Mechanisms of olfactory dysfunction in aging and neurodegenerative disorders. Ageing Res Rev 2004;3:215–32
34. Price JL. Olfaction. In: Paxinos G, Mai G, eds. *The Human Nervous System.* San Diego, CA: Elsevier Academic Press, 2004:1197–211
35. Ikemura M, Saito Y, Sengoku R, et al. Lewy body pathology involves cutaneous nerves. J Neuropath Exp Neurol 2008 In press.
36. Saito Y, Nakahara K, Yamanouchi H, et al. Severe involvement of ambient gyrus in dementia with grains. J Neuropathol Exp Neurol 2002; 61:789–96
37. Yamaguchi H, Haga C, Hirai S, et al. Distinctive, rapid, and easy labeling of diffuse plaques in the Alzheimer brains by a new methenamine silver stain. Acta Neuropathol (Berl) 1990;79:569–72
38. Gallyas F. Silver staining of Alzheimer's neurofibrillary changes by means of physical development. Acta Morphol Acad Sci Hung 1971; 19:1–8
39. Saito Y, Kawashima A, Ruberu NN, et al. Accumulation of phosphorylated alpha-synuclein in aging human brain. J Neuropathol Exp Neurol 2003;62:644–54
40. Fujiwara H, Hasegawa M, Dohmae N, et al. alpha-Synuclein is phosphorylated in synucleinopathy lesions. Nat Cell Biol 2002;4:160–64
41. McKeith IG, Galasko D, Kosaka K, et al. Consensus guidelines for the clinical and pathologic diagnosis of dementia with Lewy bodies (DLB): Report of the consortium on DLB international workshop. Neurology 1996;47:1113–24
42. McKeith IG, Dickson DW, Lowe J, et al. Diagnosis and management of dementia with Lewy bodies: Third report of the DLB Consortium. Neurology 2005;65:1863–72
43. Murayama S, Saito Y. Pathological diagnostic criteria of Lewy body dementia. In: *Symposium on Pathological Diagnosis of non-Alzheimer-type Dementia.* San Francisco, CA: XVIth International Congress of Neuropathology, 2006
44. Saito Y, Ruberu NN, Sawabe M, et al. Lewy body-related alpha-synucleinopathy in aging. J Neuropathol Exp Neurol 2004;63:742–49
45. Braak H, Braak E. Neuropathological stageing of Alzheimer-related changes. Acta Neuropathol (Berl) 1991;82:239–59
46. Saito Y, Ruberu NN, Sawabe M, et al. Staging of argyrophilic grains: An age-associated tauopathy. J Neuropathol Exp Neurol 2004;63:911–18
47. Murayama S, Saito Y. Neuropathological diagnostic criteria for Alzheimer's disease. Neuropathology 2004;24:254–60
48. The National Institute on Aging and Reagan Institute Working Group on Diagnostic Criteria for the Neuropathological Assessment of Alzheimer's Disease. Consensus recommendations for the postmortem diagnosis of Alzheimer's disease. Neurobiol Aging 1997;18:S1–2
49. Jellinger KA. Dementia with grains (argyrophilic grain disease). Brain Pathol 1998;8:377–86
50. Jellinger KA, Bancher C. Senile dementia with tangles (tangle predominant form of senile dementia). Brain Pathol 1998;8:367–76
51. Hauw JJ, Daniel SE, Dickson D, et al. Preliminary NINDS neuropathologic criteria for Steele-Richardson-Olszewski syndrome (progressive supranuclear palsy). Neurology 1994;44:2015–19
52. Roman GC, Tatemichi TK, Erkinjuntti T, et al. Vascular dementia: Diagnostic criteria for research studies. Report of the NINDS-AIREN International Workshop. Neurology 1993;43:250–60
53. Hasegawa M, Jakes R, Crowther RA, et al. Characterization of mAb AP422, a novel phosphorylation-dependent monoclonal antibody against tau protein. FEBS Lett 1996;384:25–30
54. Tsuboi Y, Wszolek ZK, Graff-Radford NR, et al. Tau pathology in the olfactory bulb correlates with Braak stage, Lewy body pathology and apolipoprotein epsilon4. Neuropathol Appl Neurobiol 2003;29:503–10
55. Folstein MF, Folstein SE, McHugh PR. "Mini-mental state." A practical method for grading the cognitive state of patients for the clinician. J Psychiatr Res 1975;12:189–98
56. Hasegawa KI, Inoue K, Moriya K. An investigation of dementia rating scale for the elderly. Seishin Igaku 1974;16:965–69
57. Lawton MP, Brody EM. Assessment of older people: Self-maintaining and instrumental activities of daily living. Gerontologist 1969;9:179–86
58. Hughes CP, Berg L, Danziger WL, et al. A new clinical scale for the staging of dementia. Br J Psychiatry 1982;140:566–72
59. McKhann G, Drachman D, Folstein M, et al. Clinical diagnosis of Alzheimer's disease: Report of the NINCDS-ADRDA Work Group under the auspices of Department of Health and Human Services Task Force on Alzheimer's Disease. Neurology 1984;34:939–44
60. Hixson JE, Vernier DT. Restriction isotyping of human apolipoprotein E by gene amplification and cleavage with HhaI. J Lipid Res 1990;31: 545–58
61. Murayama S, Saito Y, Kanemaru K, Tokumaru A, Ishii K, Sawabe M. Establishment of brain bank for aging research [In Japanese]. Nippon Ronen Igakkai zasshi 2005;42:483–89
62. Hoogland PV, Huisman E. Tyrosine hydroxylase immunoreactive structures in the aged human olfactory bulb and olfactory peduncle. J Chem Neuroanat 1999;17:153–61
63. Kosaka K, Yoshimura M, Ikeda K, et al. Diffuse type of Lewy body disease: Progressive dementia with abundant cortical Lewy bodies and senile changes of varying degree—a new disease? Clin Neuropathol 1984;3:185–92
64. Doty RL, Riklan M, Deems DA, et al. The olfactory and cognitive deficits of Parkinson's disease: Evidence for independence. Ann Neurol 1989;25:166–71
65. Postuma RB, Lang AE, Massicotte-Marquez J, et al. Potential early markers of Parkinson disease in idiopathic REM sleep behavior disorder. Neurology 2006;66:845–51
66. Hubbard PS, Esiri MM, Reading M, et al. Alpha-synuclein pathology in the olfactory pathways of dementia patients. J Anat 2007;211:117–24
67. Hawkes CH, Del Tredici K, Braak H. Parkinson's disease: A dual-hit hypothesis. Neuropathol Appl Neurobiol 2007;33:599–614
68. Hawkes CH. Parkinson's disease and aging: Same or different process? Mov Disord 2008;23:47–53
69. Prediger RD, Batista LC, Medeiros R, et al. The risk is in the air: Intranasal administration of MPTP to rats reproducing clinical features of Parkinson's disease. Exp Neurol 2006;202:391–403
70. Marui W, Iseki E, Kato M, et al. Pathological entity of dementia with Lewy bodies and its differentiation from Alzheimer's disease. Acta Neuropathologica 2004;108:121–28
71. Iseki E, Marui W, Kosaka K, et al. Frequent coexistence of Lewy bodies and neurofibrillary tangles in the same neurons of patients with diffuse Lewy body disease. Neurosci Lett 1999;265:9–12
72. Fujishiro H, Tsuboi Y, Lin WL, et al. Colocalization of tau and alpha-synuclein in the olfactory bulb in Alzheimer's disease with amygdala Lewy bodies. Acta Neuropathol (Berl) 2008;116:17–24
73. Kordower JH, Chu Y, Hauser RA, et al. Lewy body-like pathology in long-term embryonic nigral transplants in Parkinson's disease. Nat Med 2008;14:504–6
74. Li JY, Englund E, Holton JL, et al. Lewy bodies in grafted neurons in subjects with Parkinson's disease suggest host-to-graft disease propagation. Nat Med 2008;14:501–3
75. Braak H, Rub U, Gai WP, et al. Idiopathic Parkinson's disease: Possible routes by which vulnerable neuronal types may be subject to neuroinvasion by an unknown pathogen. J Neural Transm 2003;110:517–36
76. Braak H, Del Tredici K. Assessing fetal nerve cell grafts in Parkinson's disease. Nat Med 2008;14:483–85

Biomedical Research 30 (4) 227-233, 2009

Elevated levels of 4-hydroxynonenal-histidine Michael adduct in the hippocampi of patients with Alzheimer's disease

Mitsugu FUKUDA[1], Fumihisa KANOU[2], Nobuko SHIMADA[1], Motoji SAWABE[3], Yuko SAITO[3, 4], Shigeo MURAYAMA[4], Masakatsu HASHIMOTO[2], Naoki MARUYAMA[1] and Akihito ISHIGAMI[1, 5]

[1] Aging Regulation, Tokyo Metropolitan Institute of Gerontology, Tokyo, Japan; [2] Shima Laboratories, Tokyo, Japan; [3] Department of Pathology, Tokyo Metropolitan Geriatric Hospital, Tokyo, Japan; [4] Department of Neuropathology, Tokyo Metropolitan Institute of Gerontology, Tokyo, Japan; and [5] Department of Biochemistry, Faculty of Pharmaceutical Sciences, Toho University, Chiba, Japan

(Received 7 May 2009; and accepted 12 June 2009)

ABSTRACT

Alzheimer's disease (AD) is among the most common causes of progressive cognitive impairment in humans and is characterized by neurodegeneration in the brain. Lipid peroxidation is thought to play a role in the pathogenesis of AD. 4-hydroxynonenal (HNE) results from peroxidation of polyunsaturated fatty acids and it in turn gives evidence of lipid peroxidation *in vivo*. HNE reacts with protein histidine residue to form a stable HNE-histidine Michael adduct. To clarify the influence of lipid peroxidation on the pathogenesis of AD, we measured HNE-histidine Michael adduct in hippocampi from four AD patients and four age-matched controls by means of semiquantitative immunohistochemistry using a specific antibody to cyclic hemiacetal type of HNE-histidine Michael adduct. This antibody does not react with the ring-opened form of HNE-histidine Michael adduct and the pyrrole form of HNE-lysine Michael adduct. The HNE adduct was detected in the hippocampi of both AD and control donors, especially in the CA2, CA3 and CA4 sectors. Immunoreactive intensity of HNE adduct in these sectors were significantly higher in AD patients than in the controls. The HNE adduct was found in the perikarya of pyramidal cells in the hippocampus. These results show that the hippocampi of patients with AD undergo lipid peroxidation and imply that this activity underlies the production of cytotoxic products such as HNE that are responsible for the pathogenesis of AD.

The progressive cognitive impairment of Alzheimer's disease (AD) is associated with neuronal loss as well as the formation of neurofibrillary tangles (NFTs) and senile plaques in the brain (25). Free radical-mediated oxidative damage, energy depletion, deposition of amyloids and NFTs, excitotoxicity, and vascular endothelial cell damage are all thought to participate in the pathogenesis of AD (13). Oxygen-derived free radicals, byproducts of respiration, cause oxidative damage to cellular biomolecules including lipids, proteins and nucleic acids. The brain seems to be especially vulnerable to lipid peroxidation by free radicals, because it consumes approximately one-fifth of humans' oxygen intake, has a relative paucity of antioxidant systems and contains high concentrations of polyunsaturated fatty acids (PUFAs) (11). Lipid peroxidation results in structural damage to membranes and generation of secondary products such as reactive aldehydes

Address correspondence to: Akihito Ishigami, Ph.D. Department of Biochemistry, Faculty of Pharmaceutical Sciences, Toho University, Miyama 2-2-1, Funabashi, Chiba 274-8510, Japan
Tel/Fax: +81-47-472-1536
E-mail: ishigami@phar.toho-u.ac.jp

Abbreviations used: AD, Alzheimer's disease; DAB, 3,3'-diaminobenzidine tetrahydrochloride; HNE, 4-hydroxynonenal; MAP2, microtubule-associated protein 2; NFT, neurofibrillary tangle; PBS, phosphate buffered saline; PUFAs, polyunsaturated fatty acids.

that modify proteins and nucleic acids (5). Therefore, as reported, lipid peroxidation in the brains of AD patients not only harms cells but increases levels of such peroxidation products as thiobarbituric acid-reactive substances (10), acrolein-deoxyguanosine adducts (9), and cytotoxic compounds such as acrolein (12) and 4-hydroxynonenal (HNE) (17).

Lipid peroxidation propagates itself by autoxidation initiated by free radicals and produces considerable amounts of secondary products before the process terminates (21). These well-known secondary products include reactive aldehydes, such as acrolein, malondialdehyde, HNE, and 4-hydroxyhexenal (5). HNE is product that results from the lipid peroxidation of n-6 PUFAs, *e.g.*, linoleic acid and arachidonic acid (5). Because the brain is rich in arachidonic acid (29), lipid peroxidation tends to produce HNE at that site. These substances then react with proteins, nucleic acids and small molecules such as glutathione in cells and eventually impair normal biological functions of the essential components (5). Indeed, HNE is cytotoxic for cultured neuronal cells (2, 5, 8, 15). Therefore, HNE might induce neuronal cell death and neurodegeneration in patients with AD.

Measuring the exact quantity of HNE *in vivo* is difficult, since they are rapidly consumed when their chemically active aldehyde reacts with such cellular components as glutathione, proteins and nucleic acids (5). HNE reacts with lysine, histidine and cysteine residues in proteins to form Michael adducts and also Schiff base products (lysine ε-NH_2). When HNE reacts with proteins, HNE-histidine Michael adduct is a major product that develops in the cyclic hemiacetal form (3, 27). Because the cyclic hemiacetal form of HNE is relatively stable (5), the detection of HNE Michael adduct is considered a reliable index of lipid peroxidation. This property enabled us to measure HNE-histidine Michael adduct using the specific antibody to cyclic hemiacetal type of HNE-histidine Michael adduct.

To clarify the influence of lipid peroxidation on the pathogenesis of AD, we directly assessed the cyclic hemiacetal type of HNE-histidine Michael adduct in brain specimens from AD subjects and age-matched controls. As a result, the HNE adduct was detected in the hippocampi of both groups, especially the CA2, CA3 and CA4 sectors. The important difference was significantly higher levels of the HNE adduct in the brains of patients with AD. This is the first report of specific antibody usage for direct detection of HNE-histidine Michael adduct in the cyclic hemiacetal form within hippocampi from humans with AD.

MATERIALS AND METHODS

Human subjects. All clinical data from patients and information at autopsies from four patients with AD (two women and two men) and four (one women and three men) normal (no AD), age-matched subjects who died during the last several decades were retrieved from the autopsy database of the Department of Tokyo Metropolitan Geriatric Hospital, Tokyo, Japan. Brain specimens were registered in the Brain Bank for Aging Research (BBAR) organized by Tokyo Metropolitan Geriatric Hospital and Tokyo Metropolitan Institute of Gerontology (TMIG). Brain specimens used in this study were from patients clinically diagnosed as having AD-positive and control subjects without any sign of AD. All AD patients met accepted criteria for the neuropathologic diagnosis of AD based on the National Institute of Aging (NIA)-Reagan Institute Criteria for the Neuropathological Diagnosis of AD (1997) (1), combining abundant neuritic plaques in the neocortex (definite AD with consortium to establish a registry for AD criteria) and a profusion of NFTs in the limbic and neocortical areas (Braak and Braak staging, VI). Normal subjects used as controls were individuals with no history of dementia or other neurological disorders. Neuropathologic evaluation of control brains revealed only age-associated gross and histopathologic alterations (Braak and Braak NFT staging, I and SP stage, 0 or A). The subjects' demographic data are summarized in Table 1. The human studies were approved by Ethics Committees of TMIG and the Tokyo Metropolitan Geriatric Hospital.

Immunohistochemistry. Specimens were taken from the hippocampus and fixed with 4% paraformaldehyde in this study. Paraffin-embedded hippocampal sections were deparaffinized, rehydrated with xylene, alcohol and phosphate buffered saline (PBS), microwaved for 5 min in boiling 10 mM citrate buffer, pH 6.0, and immersed in 3% H_2O_2 in methanol for 15 min to reduce endogenous peroxidase activity. After blocking treatment with 10% non-immune goat serum in PBS (blocking solution) for 60 min at room temperature, the specimens were incubated with the primary antibodies overnight at 4°C and then for 60 min at room temperature. Mouse monoclonal antibody against HNE-histidine Michael adduct which was specific for their cyclic hemiacetal form was purchased from NOF Corporation (Tokyo,

Japan), and was used at a dilution of 1 : 100 with a blocking solution. After adequate washing with PBS, specimens were incubated with the secondary antibody (goat anti-mouse IgG conjugated with horseradish peroxidase, Simplestain MAX-PO (M); Nichirei Biosciences Inc., Tokyo, Japan) for 60 min at room temperature. Thorough washing with PBS and incubation with 0.02% 3,3'-diaminobenzidine tetrahydrochloride (DAB) (Wako Pure Chemical Industries, Osaka, Japan) followed for 10 min at room temperature to visualize HNE-adduct. For double-labeling immunohistochemistry, two primary antibodies were used: anti-microtubule-associated protein 2 (MAP2) and the anti-HNE-histidine adduct antibodies. Tissue specimens were incubated with the anti-MAP2 antibody (1 : 500 dilution; Chemicon AB5622, rabbit polyclonal antibody; Billerica, MA, USA) to confirm pyramidal neurons, and then with Simplestain AP (R) as a secondary antibody conjugated with alkaline phosphatase. The alkaline phosphatase activity was visualized with Vector Red Alkaline Phosphatase Substrate Kit I (Vector Laboratories, Burlingame, CA, USA). Subsequently, the specimens were incubated with the anti-HNE adduct antibody as mentioned above. Hematoxylin was used for counter staining. The antibody used against HNE-histidine Michael adduct is specific for their cyclic hemiacetal form and does not react with the ring-opened form of HNE-histidine Michael adduct and the pyrrole form of HNE-lysine Michael adduct (26).

The four hippocampal sectors (CA1 through CA4) were delineated and cells that had a large nucleus containing a clearly visible nucleolus in these sectors were referred to pyramidal cells according to the description of Mani *et al.* (14). Immunoreactive intensity of the HNE-Michael adduct was assessed by measuring 20 fields of hippocampal sectors in the specimens under a 40 × objective microscopic field. The extent of staining intensity in pyramidal cells was classified into the following two grades: Pyr-small (small staining size less than half of the pyramidal cell nucleus) and Pyr-large (large staining size more than half of the pyramidal cell nucleus). The extent of staining intensity in non-pyramidal cells was also classified into the following two grades: Non-small (small staining size less than the cell nuclei) and Non-large (large staining size more than the cell nuclei). The percent ratio of these grades in each sector was calculated by following formulation: percent of Pyr-small = (numbers of Pyr-small grade / (numbers of Pyr-small grade + Pyr-large grade)) × 100; percent of Pyr-large = (numbers of Pyr-large grade / (numbers of Pyr-small grade + Pyr-large grade)) × 100; percent of Non-small = (numbers of Non-small grade / (numbers of Non-small grade + Non-large grade)) × 100; and percent of Non-large = (numbers of Non-large grade / (numbers of Non-small grade + Non-large grade)) × 100.

Statistical analysis. The results are expressed as mean ± SEM. Statistical analyses were conducted by using Graphpad Prism 4 software (version 4.0, Graphpad Software Inc., San Diego, CA, USA). Significance was defined as a P value less than 0.05.

RESULTS

Clinical features of subjects

The subjects' demographic data are summarized in Table 1. The mean ages of the AD group and the control group were 86 and 78 years, respectively, and there was no significant difference between these two groups (*t-test*, two-sided). Neither brain weight, gender, nor postmortem interval differed significantly between the two groups according to a *t-test* (two-sided), Fisher's exact test, or *t-test* (two-sided), respectively.

HNE Michael adduct in the hippocampi from AD patients and non-AD controls

HNE Michael adduct in the hippocampi was detected in all specimens from both AD and controls. Especially, CA2–4 sectors contained an abundance of the HNE adduct compared with the adjacent CA1 sector (Fig. 1B and Table 2).

HNE Michael adduct immunoreactivity was seen

Table 1 *Demographic data for AD subjects and controls*

	Age (yr)	PMI (h)	Gender	BW (g)	Braak stage	
					NFT	SP
AD	86 ± 3	10.0 ± 0.1	2 M/2 F	1,110 ± 52	VI (4)	C (4)
Controls	78 ± 2	4.4 ± 2.5	3 M/1 F	1,241 ± 67	I (4)	0 (4)

Data are expressed as mean ± SEM. Parentheses indicate the number of subject. AD, Alzheimer disease; PMI, postmortem interval; h, hour; BW, brain weight; g, gram; yr, year; NFT, neurofibrillary tangle; SP, senile plaque